Effect of Time Scale on Analysis of PV System Performance

3 authors, including:

SANDIA REPORT
SAND2012-1099
Unlimited Release
Printed February 2012

Effect of Time Scale on Analysis of PV System Performance

Clifford W. Hansen, Joshua S. Stein, and Daniel Riley

Sandia National Laboratories

Effect of Time Scale on Analysis of PV System Performance

Clifford W. Hansen, Joshua S. Stein, and Daniel M. Riley
Photovoltaics and Distributed Systems Integration
Sandia National Laboratories
P.O. Box 5800
Albuquerque, New Mexico 87185-1033

Abstract

Power from photovoltaic systems can be calculated from measurements of weather data such as irradiance, air temperature and wind speed. Weather measurements are generally obtained as averages over time intervals ranging from a few seconds to as long as an hour. We examine the effects on estimates of photovoltaic power system power and energy of using weather measurements averaged over time intervals of various lengths.

We found that, in general, average power is overestimated and the distribution of power is narrowed when time-averaged weather is used. The largest changes in power, i.e., ramp rates, are reduced. We also found that energy calculated from time-averaged weather is subject to error that increases as the averaging interval lengthens; at hourly averaging intervals, for a representative system in Albuquerque, NM, absolute error in energy may be as large as 2%. Hourly energy error depends in a complex manner on the time of year and the power system's location.

We show that error in annual energy can be predicted from the frequency of clear-sky conditions and the degree of non-linearity in the photovoltaic module's response to increasing irradiance. Error in annual energy ranges from -0.3% for locations where clear-sky conditions dominate, to +2.0% for locations with variable irradiance conditions and for a module with significantly non-linear response.

We show that errors in energy are significantly reduced when the time interval between weather measurements is shortened. For example, reducing the weather-averaging interval from one hour to 15 minutes generally reduces the error in energy by a factor of 10. Consequently, for analysis of energy produced from photovoltaic systems, we recommend use of weather data at a time interval of 15 minutes or less.

ACKNOWLEDGMENTS

CONTENTS

FIGURES

TABLES

Nomenclature

AC	Alternating current
AMa	Absolute air mass
AOI	Angle of incidence
DC	Direct current
DOE	Department of Energy
DHI	Diffuse horizontal irradiance
DNI	Direct normal irradiance
GHI	Global horizontal irradiance
kWh	Kilowatt-hour
MIDC	Measurement and Instrumentation Data Center
NREL	National Renewal Energy Laboratory's
PV	Photovoltaic
SNL	Sandia National Laboratories
STC	Standard test condition

1. INTRODUCTION

Power from photovoltaic (PV) systems can be calculated from measurements of weather data such as irradiance, air temperature and wind speed. Weather measurements are generally obtained as averages over time intervals ranging from a few seconds to as long as an hour. We examine the effects on estimates of PV power system performance of using weather measurements averaged over time intervals of various lengths.

We use common modeling practices to calculate PV module performance with the Sandia Array Performance Model [1]. We calculate power at three-second and one-minute intervals from weather data measured in Albuquerque, NM, Las Vegas, NV, and Lanai, HI, and also calculate power at longer time scales using time-averages of the same weather data. We compare results calculated at different averaging intervals to examine the effect of time-averaging on the distribution of power, variability in power, and energy from the PV system.

In Section 2.3 we examine the effects of using time-averaged weather on the calculated distribution of power. In particular, we investigate the effects on the average (over time) power, the standard deviation and percentiles of the distribution of power, and on the ramp rates of changes in power.

In Section 2.4, we analyze the potential error in energy resulting from the integration of power calculated with time-averaged weather. We investigate the sources of error, the dependence of error on irradiance conditions and PV module characteristics, and the potential for development of error correction methods. From estimates of PV system performance at different locations, we quantify a range of values for the error in aggregate annual energy that results from the use of time-averaged weather.

In Section 2.5, we discuss the effect of using time-averaged weather on a PV system design, in particular, the selection of the inverter size for a PV system.

Finally, we conclude with a brief survey of the effect of time-averaged weather on the representation of a PV system in analyses of the electric grid (Section 2.6).

2. ANALYSIS

Photovoltaic (PV) system power is generally estimated by a mathematical model. Several models with different formulations and implementation in software are available [1, 2, 3, 4]. However, all performance models require irradiance as an input, and most require other weather quantities such as air temperature and wind speed.

Models for power generally assume that the PV system responds rapidly to changes in external variables, and thus power is calculated at discrete times using instantaneous weather values. Weather values are generally obtained as time averages, although the time interval over which measurements are averaged varies greatly, from a few seconds to as long as an hour.

The analysis presented in this section examines the effects on model results due to using different time scales for the weather variables. We first establish notation, then discuss in turn the following calculations: estimating power output; estimating energy; determining power quality on a grid with connected PV; as well as implication for PV system design.

2.1. Notation

The weather variables can be represented by a vector V, e.g., $V = (E_e, T, WS, \ldots)$ where E_e indicates effective irradiance (i.e., the solar radiation captured and used by the module), T indicates temperature, WS denotes wind speed, and so forth. These quantities are functions of time, indicated by $V = V(t) = (E_e(t), T(t), WS(t), \ldots)$ and typically are determined from measurements at regular intervals. For convenience, we assume the measurement interval Δt is fixed.

Let $P(t)$ denote the power (in watts) produced by the PV system at time t. The performance model used to calculate $P(t)$ can be represented as a function of the weather variables V and a fixed parameter vector S that describes the properties of the PV system, i.e.,

$$P(t) = f(V(t), S). \tag{1}$$

Because values for the weather variables V are given at a sequence of discrete times $t_0 = 0, t_1, \ldots t_k, \ldots = 0, \Delta t, \ldots, k\Delta t, \ldots$ we obtain a sequence of values for $P(t)$:

$$P(k\Delta t) = f(V(k\Delta t), S) \tag{2}$$

With this notation in hand we can readily represent statistics for the power sequence, and for results calculated using environmental variables on various time scales.

Given a weather vector V (i.e., a vector where each component $V_i = \{V_i(k\Delta t)\}$ is a time series of values for a weather variable) using a performance model (Eq. (1)) we obtain a time series of

11

power $\{P(k\Delta t)\}$, $k = 0,\ldots,N$ with the same time interval Δt as the weather variable time series. The time series in the weather vector may be summarized by averaging over intervals wider than Δt; for example, irradiance measurements may be made every three seconds but reported as one-minute averages (i.e., as the average of measurements over the preceding minute); the one-minute values may be further reduced to hourly averages. We denote the finest time interval available by Δt; power obtained using weather quantities averaged over time intervals that are multiples of this interval (i.e., at $M\Delta t$ for an integer M) is denoted by $\{P(kM\Delta t)\}$ where it should be understood that the index k takes values such that the sequence of times $kM\Delta t$ takes values in the interval $[0, N\Delta t]$. When considering averages that are calculated over blocks of time; the notation $\overline{P}(K\Delta t)$ indicates the time series of averages of $P(\Delta t)$ over blocks of length $K\Delta t$, and the notation $\overline{P}(kK\Delta t)$ indicates the kth value in this time series. The bar over $\overline{P}$ indicates an average and distinguishes $\overline{P}(K\Delta t)$ from $P(K\Delta t)$, which denotes the (un-averaged) power at time $K\Delta t$.

2.2. Weather Data and Calculation of Power

To illustrate the effects of time scale on weather variables and associated power, we use a set of concurrent weather measurements collected at Sandia National Laboratories in Albuquerque, NM in late August through early September 2008. Measurements of global horizontal irradiance (GHI), direct normal irradiance (DNI), diffuse horizontal irradiance (DHI), ambient temperature and wind speed were recorded at intervals usually ranging from 2.8 to 4 seconds. While all weather data was sampled instantaneously, some instruments respond to environmental changes with response times longer than the sampling interval, thereby introducing a smoothing or averaging effect. In particular, the irradiance instruments employed thermopile (broadband) sensors with 99% response times on the order of 13-17 seconds, and the sampled wind speed is representative of a 15 second moving average. Because measurements are not always reported at a consistent time interval of three seconds, due to data transmission timing or missing data, we regularized the weather data to three-second intervals by linearly interpolating between measurements. Regularization facilitates the calculation of time averages and of statistics that summarize the weather and resulting power data and should not adversely affect the validity of this analysis.

Measured weather data are paired with calculated values for solar azimuth and zenith angles and absolute air mass (AMa), which was calculated as $AMa = \sec(z)$ where z is the solar zenith angle ([5], Eq. 22.12). Solar angle of incidence (AOI) was then computed, assuming a PV module fixed at latitude tilt and facing southward. Figure 1 illustrates GHI, ambient temperature and wind speed measurements on August 24, 2008 (clear day) and August 15, 2008 (cloudy day), and the resulting time series of DC power calculated using the Sandia Array Performance Model [1] for a Yingli Y230 (230WDC) cSi module. Figure 2 shows the estimated power from a Yingli module for each of the sixteen selected days. The Yingli module was chosen because its performance characteristics are representative of current crystalline silicon (c-Si) PV module technology.
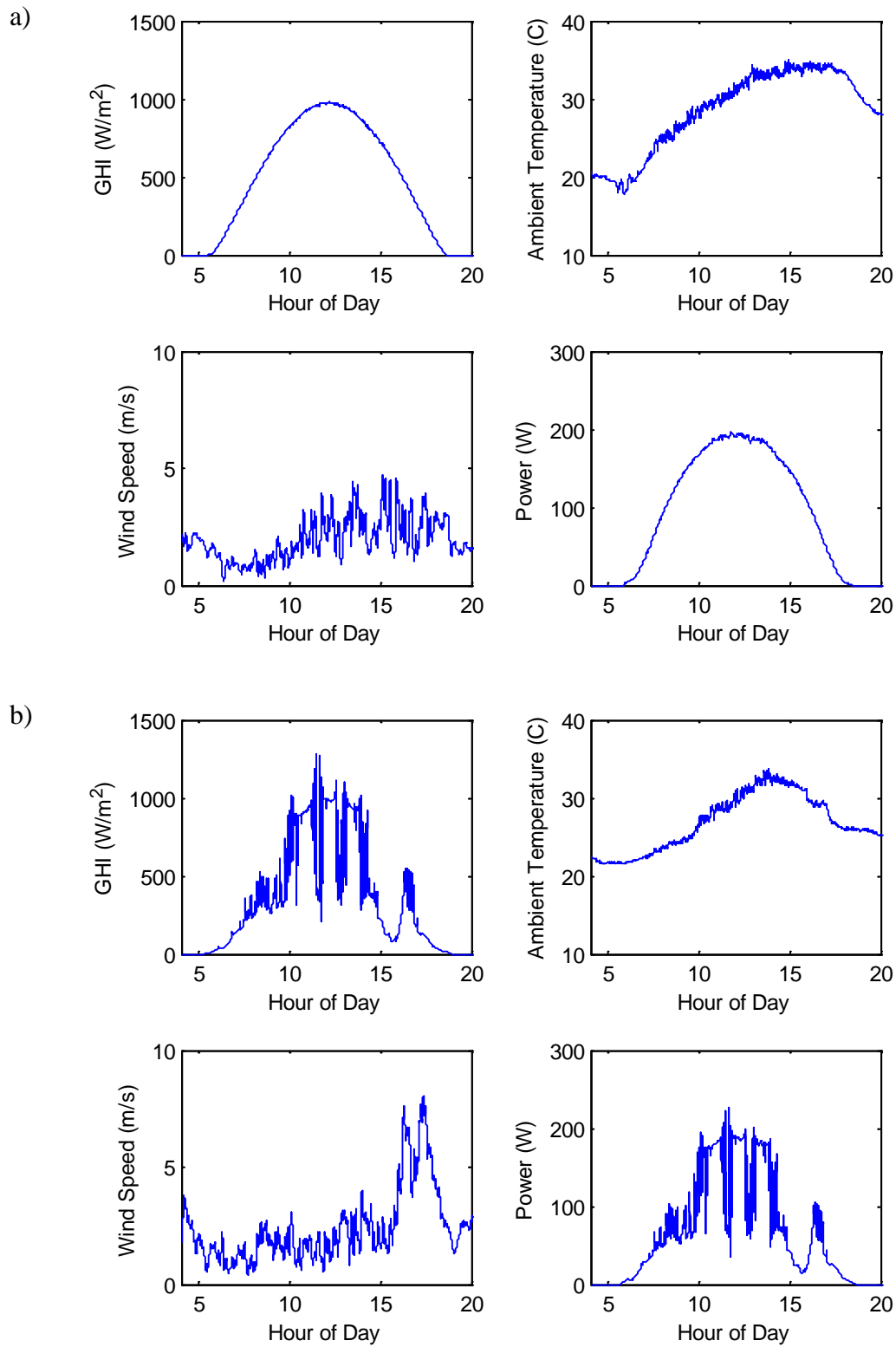
Figure 1. Example irradiance, temperature and wind speed, and corresponding power from a 230W cSi module: (a) Clear Day; (b) Cloudy Day.
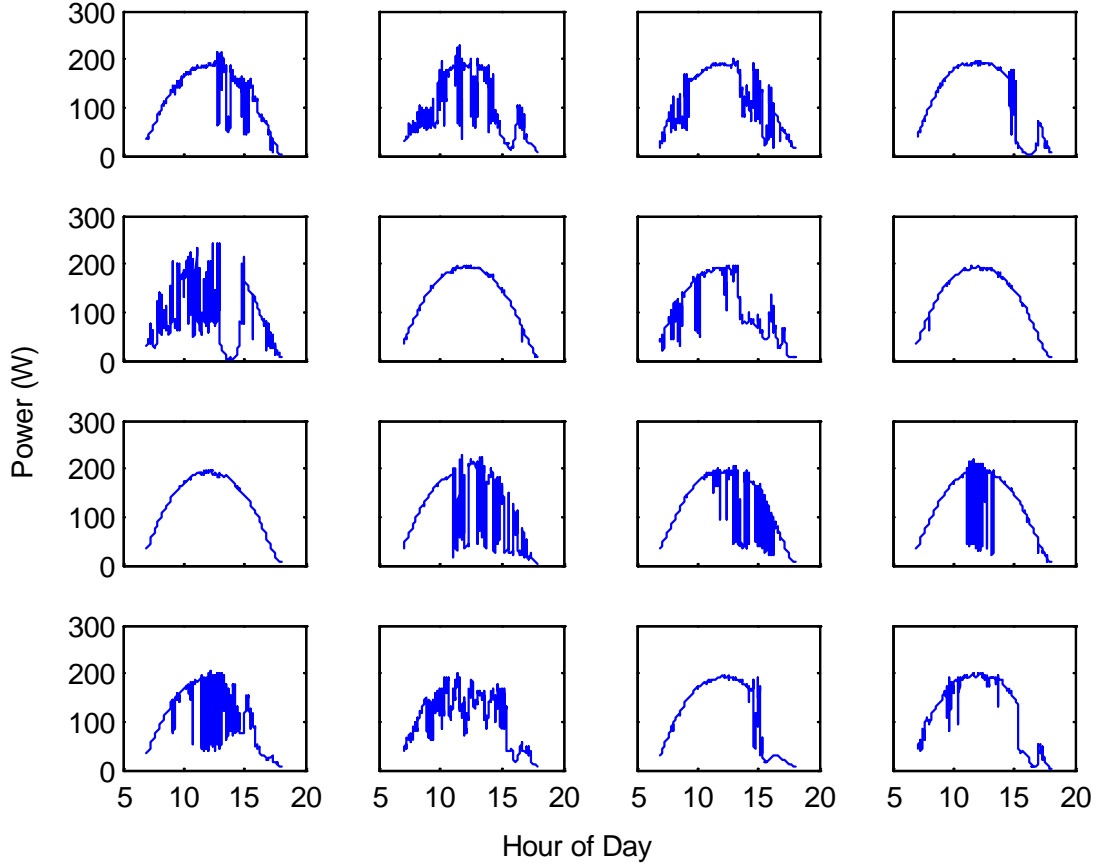
Figure 2. Estimated Power for Sixteen Days in Albuquerque, NM.

Using measured GHI and DHI, diffuse plane-of-array irradiance was estimated at three-second intervals using the King model [6]. Beam irradiance was calculated by multiplying DNI by the cosine of the angle-of-incidence (*AOI*). Module temperature was calculated from total incident irradiance, ambient temperature and wind speed using an empirical model ([1], Eq. 11), and module temperature was used to estimate cell temperature ([1], Eq. 12).

Time-averaged weather variables were then determined by averaging, over various intervals, direct normal irradiance, diffuse irradiance, and module temperature. Consistent with current practice, *AOI* and *AMa* values for each interval were taken to be equal to the value at the interval's midpoint, except for intervals during which sunrise or sunset occur. Sunrise and sunset times were determined to be when the solar elevation angle rises above zero. For time intervals containing sunrise and sunset events, *AOI* and *AMa* values were taken to be equal to the midpoint of the part of the interval with daylight. Using the time-averaged weather variables and corresponding *AOI* and *AMa* values, DC power was calculated using the Sandia Array Performance Model [1].

14

2.3. Effect of Averaging on Power Estimates

When weather variables are specified at a point in time, the power calculated at that time does not depend on the time scale of the weather vector V, because power is an instantaneous quantity. Rather, error in the calculated power depends on:

- Measurement error in the weather variables;
- Model error (misspecification) in the model used to calculate power;
- Estimation error in the parameters (i.e., the vector S) that characterize the PV system.

Discussion of the magnitudes and sources for these errors is beyond the scope of this paper; we mention only that analyses are available which report on measurement error for weather sensors [7; 8] and on model and parameter error for PV modules [9; 10].

Most often, available weather data are time-averaged measurements over the measurement interval Δt rather than instantaneous measurements at each time t_k. If the performance model is linear in each weather variable, i.e., the model has the form $P(t) = aE_e(t) + bT(t) + \dots$ where a and b are constants, then the model's average value for power, $\overline{P}(t)$, is equal to that obtained by using the average weather values:

$$\overline{P}(t) = a\overline{E_e}(t) + b\overline{T}(t) + \dots \tag{3}$$

However, PV system response is not linear in general, although for many purposes, acceptable approximations can be made by assuming linear response. Figure 3 illustrates the measured power the selected Yingli module plotted against effective irradiance (i.e., the solar radiation that is captured by the module's cells). The concave downward shape of the module's response at high levels of effective irradiance is typical of semi-conductor solar photovoltaic devices. Current generally increases proportionally with effective irradiance ([1], Eq. 1 and Eq. 2), while voltage generally increases with the logarithm of effective irradiance and decreases linearly with temperature ([1], Eq. 4), with the net effect being that power increases sublinearly with increasing effective irradiance and decreases linearly with increasing temperature. Irradiance and temperature tend to increase together, and because changes in effective irradiance have a greater effect on power than do changes in cell temperature, the net result is that power increases sublinearly with increasing effective irradiance. The curvature evident in Figure 3 reflects the combined effects of changes in both effective irradiance and temperature
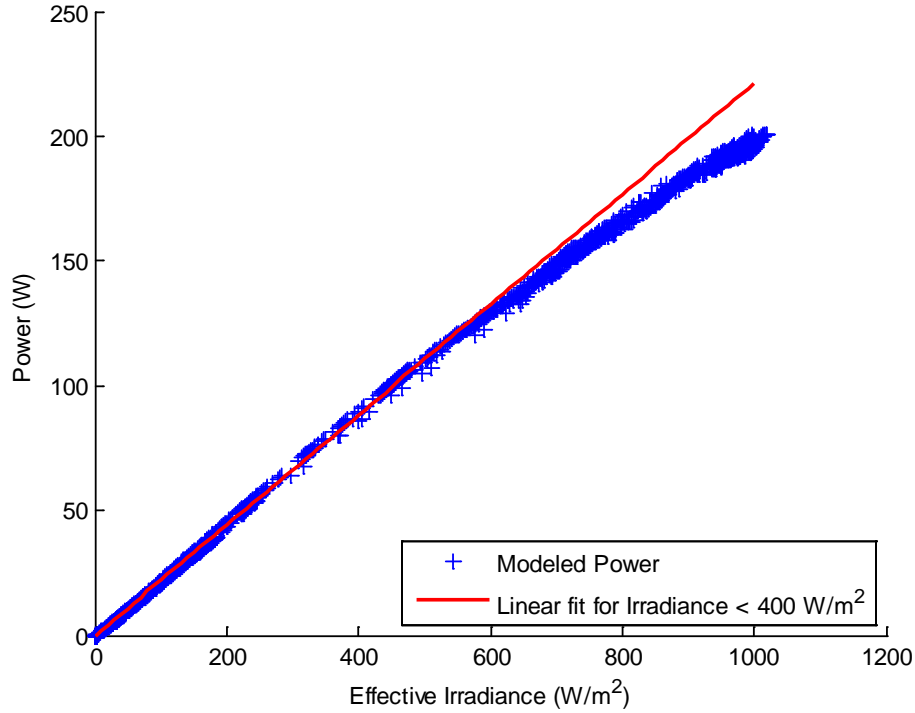
Figure 3. Module Response to Increasing Irradiance.

In the discussion that follows, we examine the effects of the time scale of the weather variables on two characteristics of the time series for power, namely: the distribution of power levels and the ramps (changes in time) of power.

2.3.1. Distribution of Power

The distribution of power $F(P)$ describes the relative frequency at which different values of power occur. Various methods are available to estimate the distribution from the time series (e.g., histograms, empirical distribution functions).

The weather variable with the strongest influence on power is irradiance, and power generally increases with increasing irradiance. Consequently, the distribution of power typically resembles the distribution of irradiance.

Many authors have described distributions of irradiance obtained from measurements at different time scales; the number of published studies decreases as the time scales decrease. Often, irradiance is normalized by the clear-sky value to obtain a clearness index, which allows observations at different latitudes and seasons to be aggregated. A summary of studies of the distributions of irradiance and of clearness indices for different time scales is found in [11], Chapter 3. Generally, distributions of daily average irradiance are unimodal with skewness that varies with geographic location, in response to the relative frequency of cloudy weather; hourly average irradiance distributions show a similar character. However, as the time scale decreases

16

towards one minute or shorter, distributions of irradiance become distinctly bimodal where the two modes result from the intermittent interposition of clouds between the sun and sensor. We suspect the time scale at which a bimodal shape emerges is the average time for a cloud to pass over the sensor but have no empirical evidence of this relationship between time scale and cloud movement.

Figure 4 illustrates histograms of irradiance measured on three-second intervals, averages of measured irradiance over five-minute and one-hour periods, and corresponding histograms of power calculated from the measured and averaged irradiance. Measurements are from 16 days in August, 2008, in Albuquerque, NM, between 7 am MST and 6 pm MST; power calculated from these irradiance measurements is illustrated in Figure 2. The bimodal character of the distribution is evident at the short (i.e., three-second and five-minute) time intervals, but appears only weakly in plots of the hourly-averaged quantities. Also, averaging reduces the extreme values of the distributions: brief excursions of irradiance above 1200 W/m^2 are indicated in the distribution of three-second irradiance averages, but are not present in the hourly averages.

Statistics summarizing the distribution of power can be affected by averaging. Table 1 lists the means, standard deviations and high quantiles for the distributions of power for averaging intervals ranging from three seconds to one hour.
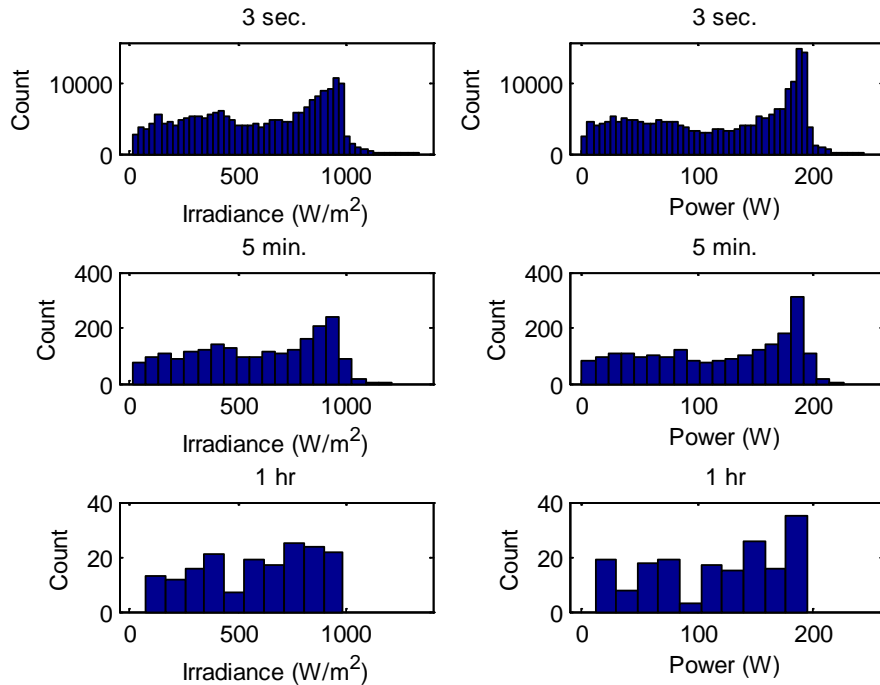
Figure 4. Distributions of Measured Irradiance and Modeled Power for Several Averaging Intervals.

Table 1. Statistics for the Distribution of Power (W) for Different Averaging Times.

	Mean	Standard deviation	50th percentile	95th percentile	99th percentile
3 sec.	116.4	62.8	125.5	193.7	206.7
1 min.	116.4	62.4	125.6	193.4	204.8
5 min.	116.6	61.4	125.5	192.6	200.0
15 min.	116.8	59.9	124.0	191.8	194.8
1 hour	117.1	56.6	126.1	191.0	194.1

The mean of the distribution of power increases with time averaged weather data, whereas the median is generally unaffected. The increase in the mean with increasing averaging time results from the non-linear response of the module (as described by the performance model) with increasing irradiance (Figure 3). When power is calculated from hourly-averaged weather, one obtains a value for power that is generally greater than the average of power computed over the same hour from weather data at shorter time intervals. More formally, because module response to effective irradiance is sublinear, if E_{e1} and E_{e2} are two irradiance values, power at the average of E_{e1} and E_{e2} will in general be greater than the average of power computed for each value of irradiance:

$$P\left(\left(\frac{E_{e1}+E_{e2}}{2},\ldots\right)\right) \geq \frac{1}{2}\left(P\left(E_{e1},\ldots\right)+P\left(E_{e2},\ldots\right)\right). \tag{4}$$

The relationship between the quantities on each side of the inequality in Eq. (4) is illustrated by Figure 5.
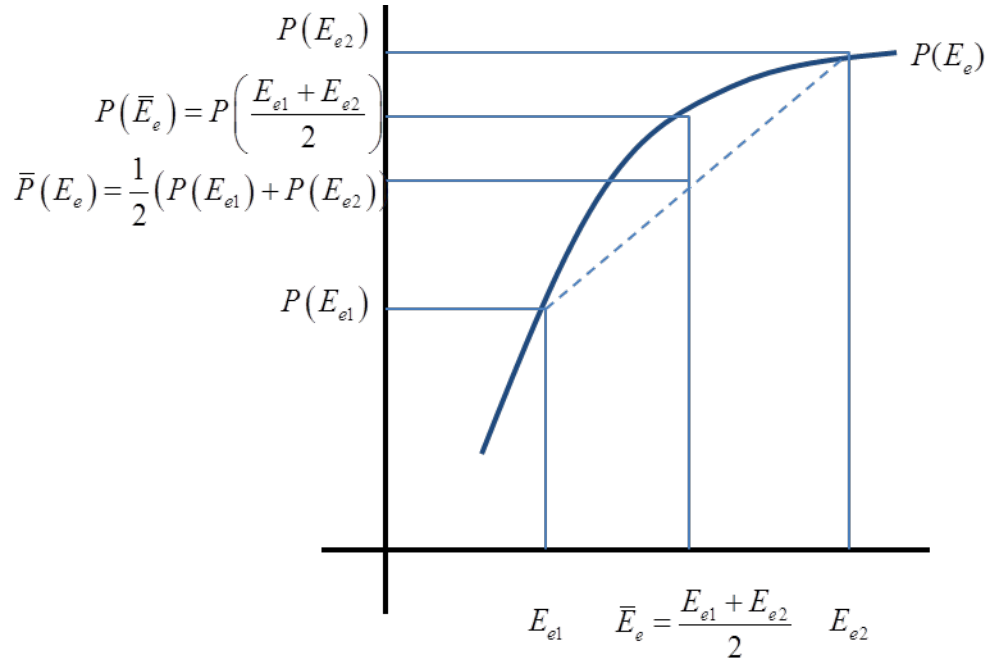
Figure 5. Illustration of Effect of Time Averaging on the Average Values for Power.

Consequently, calculating average power with averaged weather variables results in an overestimate of the average power; the overestimate is greatest for mid-day hours when irradiance is at its greatest values. If average power is calculated for a time period while irradiance is low and in this range of irradiance, module response is supralinear (i.e., power output increases more rapidly than linearly as irradiance increases), then the mean value for power for this interval of time would be underestimated from time-averaged weather variables. However, because power is generally low when irradiance is low, and low values of power have less influence on the average value for power than do high values of power, we conclude that, in general, the average value of power is likely overestimated when using time-averaged weather variables.

We expect averaging to decrease variability in the averaged data due to the removal of extreme values. Increasing averaging from three seconds to one hour reduces the standard deviation by about 10%, the 95th percentile by roughly 2%, and the 99th percentile by roughly 7%. The reductions indicate that the distribution for power calculated from averaged weather data is somewhat narrower (i.e., is less variable) as compared to the distribution for power at short time scales.

We conclude that averaging weather data has two primary effects on the distribution of power from a PV system: mean values are likely overestimated because module response is sublinear at high irradiance levels; and extreme values are removed and variability is reduced.

Other authors have observed similar effects on model results from using time-averaged model inputs. For a representative crystalline Si module, Riley et al. [12] examined the effects of time-averaging on calculated power. They quantified the effects by calculating the mean absolute error (MAE) and root mean squared deviation (RMSD) between the time series of three-second power, and the time series of power averaged over intervals, where within an interval the power was assumed to be constant at the average value. They found that increasing the averaging interval increases the MAE and RMSD between three-second time series and averaged time series, indicating a widening discrepancy between the model results, by amounts similar to the percentage changes shown in Table 1. However, their work examines statistics that summarize the differences between time series, whereas we compare statistics for the power distributions (i.e., the marginal distributions of the time series). Our results can be compared qualitatively, but not quantitatively, to those in Riley et al. [12].

Changes to the distribution of power may propagate to changes in other quantities, such as energy, that are calculated from power. For example, if selection of system components (e.g., inverters) is based on extreme values of power, system performance can be affected by time averaging. A less variable distribution of power may result in underestimating the effects of PV output variability on the electrical system to which it is connected. In Section 2.3.2, we further examine the effect of time-averaging on variability in power output as measured by the rate of change of power (i.e., ramps). In Section 2.4 we analyze the effects of time-averaging on the calculation of energy. In Section 2.6 we examine the loss of total energy production due to inverter clipping that may occur if the inverter capacity is determined by a percentile of estimated power and power is, in turn, determined from time-averaged weather data.

2.3.2. Variability in Power

The power output of a PV system is inherently variable due to natural variability in weather, and in particular, irradiance. The magnitude of changes in power, the time rate of change (e.g., kW/min) and the frequency with which changes occur are all of interest.

A time series of changes in power, $\Delta P(k\Delta t)$, is obtained from the time series of power $P(k\Delta t)$ by differencing consecutive power values:

$$\Delta P(k\Delta t) = P(k\Delta t) - P\big((k-1)\Delta t\big). \tag{5}$$

The time series of changes in power is converted to a time series of ramp rates by dividing by time interval length:

$$R(k\Delta t) = \frac{1}{\Delta t}\Delta P(k\Delta t) \tag{6}$$

so that ramp rates can be compared for different time intervals. Visually, the time series of ramp rates is the time series of the slopes of line segments connecting consecutive power values.

Time series of ramp rates at more coarse time scales (i.e., those which result from a time series of time-averaged power) are inherently less variable than are time series of ramp rates at finer time scales. The reduction in variability results because the power values at coarser time scales are averages and will naturally cluster closer to the overall average value of power than power values that are not time averaged; thus changes between power values will occur at lower rates.

Figure 6 illustrates the reduction in variability (quantified here by the cumulative distribution of ramp rates) for various averaging intervals. Ramp rates in Figure 6 are aggregated for all times between 7 am and 6 pm over all 16 days with measurements. For relative short averaging times (e.g., one minute) large ramps are possible (e.g., exceeding 50 W/min) and the largest ramps effectively represent transition between full power and minimal system power over a single time interval. As averaging interval increases, the largest ramps are smoothed out of the time series, and at hourly averages, changes in power occur at relatively slow rates (e.g., at a maximum rate of 2 W/min in the ramp rates resulting from 60-minute averaging).
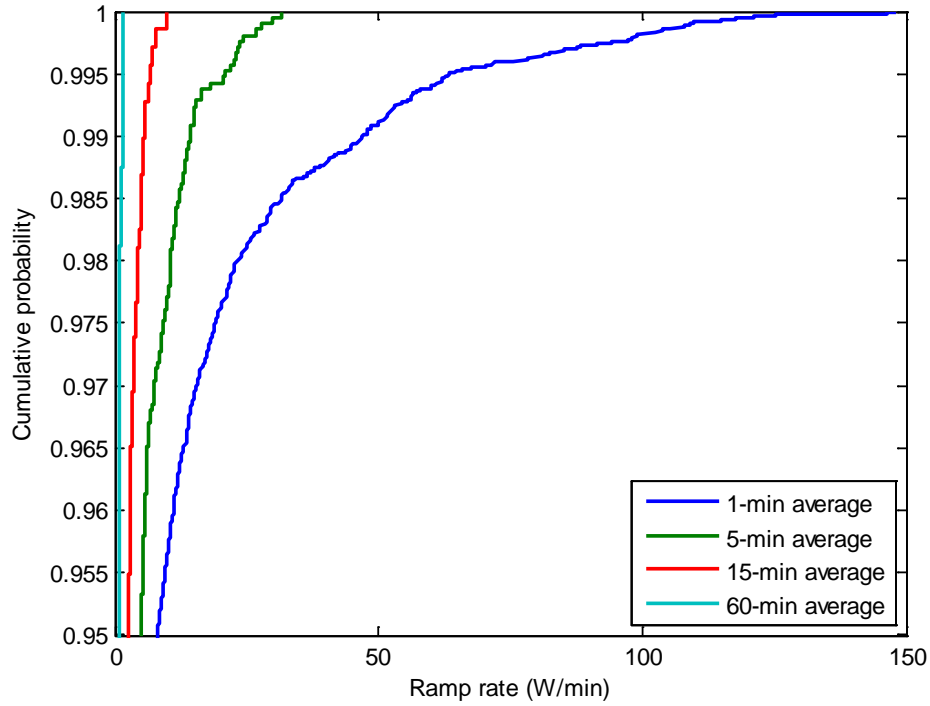
Figure 6. Effect of Time Averaging on Changes in Power Output.

Ramps in grid-connected PV power output can affect voltages and frequency of power on the grid. Grid operators must maintain system voltage and frequency within specified tolerances, and so conduct grid integration studies to quantify the effects of variability in PV systems and to determine appropriate mitigation measures. In these studies, it is often the extremes of the ramp rate values that are of interest. Because time-averaging affects the tails of the distribution of PV power ramp rates in a dramatic fashion, it is essential to select a time scale for weather data that results in an accurate representation of power ramps at the time scales appropriate to the study's objectives.

2.4. Estimating Total Energy

The total energy produced from a PV system over a period of time (e.g., annually) is of primary interest when considering the economic value of the system. Estimates of energy can be affected by the numerical method used to calculate energy, and statistics for energy can be biased as a result of averaging the underlying environmental variables.

Energy is the integral of power over time. Because power is estimated at a discrete sequence of time points, more coarse time scales (i.e., larger values for Δt) intuitively suggest less accuracy in the estimation of energy. Moreover, calculating energy requires selecting a method of numerically integrating the time series of power, which also contributes to error in the estimate of energy. We first compare the values of energy calculated using different time scales and

different methods for numerical integration to determine the error in estimated energy arising from its numerical calculation.

2.4.1. Numerical Error in Calculation of Energy

Integration over time implicitly entails choice of a method to approximate power within each interval. If energy is estimated by a straightforward summation of power over time, weighted by the interval length, i.e.,

$$E = \Delta t \times \sum_{k=0}^{N-1} P\left(t_k^*\right) \tag{7}$$

where t_k^* is a value in the time interval $[t_k, t_{k+1}]$ (i.e., $t_k \le t_k^* \le t_{k+1}$), the result is equivalent to assuming that over each interval $[t_k, t_{k+1}]$ power remains constant at the selected value $P\left(t_k^*\right)$. Here we adopt the convention that the time series of interest is indexed from 0 to N, and thus the upper limit $N-1$ in the sum in Eq. (7) ensures that power is estimated over the time period $[t_0, t_N]$. Rearranging the terms in Eq. (7) shows the relationship between the summation and the integral defining energy:

$$E = \int_{t_0}^{t_N} P(t)\, dt \approx \sum_{k=0}^{N-1} P\left(t_k^*\right) \times \Delta t = \Delta t \times \sum_{k=0}^{N-1} P\left(t_k^*\right) \tag{8}$$

The approximation in Eq. (8) is known as the rectangle or midpoint integration method, and is one of the simplest methods of integration. The rectangle method is most suited to calculation of energy when power is estimated as a representative value for each $[t_k, t_{k+1}]$, as may be the case when using weather values that have been averaged over intervals. The accuracy of Eq. (8) depends on the accuracy of the representative values $P\left(t_k^*\right)$, which can be assumed to improve as the time interval decreases.

When power is known at the interval endpoints, rather than as representative values for intervals, other assumptions can be made regarding the values of power interior to each time interval. The simplest assumption is that power is constant at $P(t_k)$ over the interval $[t_k, t_{k+1}]$; under this assumption energy is calculated using Eq. (8) by setting $P\left(t_k^*\right) = P(t_k)$. This method is known as the left-endpoint rule for numerical integration and is one of the simplest yet least accurate methods.

Other assumptions may produce more accurate estimates of energy from end-point values with little added complexity. For example, one may assume that power changes linearly from $P(t_k)$ to $P(t_{k+1})$ over each interval $[t_k, t_{k+1}]$. This assumption is implemented by using the trapezoid rule for numerical integration:

$$E \approx P(t_0)\frac{\Delta t}{2} + \sum_{k=1}^{N-1}\left(P(t_k)\times\Delta t\right) + P(t_N)\frac{\Delta t}{2}. \tag{9}$$

Integration by Eq. (9) is essentially the same as integration by Eq. (8) when the representative quantity is chosen as the average over each interval. Other methods can be used to approximate power within each interval $[t_k, t_{k+1}]$ (e.g., cubic spline interpolation) which, if chosen, are implemented by corresponding numerical integration rules (e.g., Simpson's 3/8 rule).

For the power illustrated in Figure 2, which is computed at a time interval of 3 seconds, we calculated energy using several different numerical integration schemes, to illustrate the potential error introduced by the numerical integration schemes. The midpoint, left-endpoint, trapezoid and Simpson's 3/8 rules all yielded essentially the same value for energy (20.485 kWh), which indicates that numerical error in the integration method is negligible for calculation of energy at the shortest time interval (3 seconds).

2.4.2. Effect of Averaging on Calculation of Energy

We calculated energy from power that was computed from weather variables averaged over several intervals Δt, ranging from 3 seconds to 1 hour, using the midpoint rule (Eq. (8)). We chose the midpoint method because we believe that this method is the common practice. This method regards the values of power computed from averaged weather quantities as representative of each time interval. Table 2 compares the results. Because we determined that numerical error in the integration is negligible for the shortest time interval, we may estimate the error introduced by averaging the weather variables over intervals of increasing Δt, by comparing energy estimates to those obtained with the shortest value of Δt (3 seconds).

Table 2. Comparison of Energy Calculated Using Averaged Weather Values

	Time interval (Δt) for averaging weather values				
	3 sec	15 sec	1 min	15 min	60 min
Energy (kWh)	20.485	20.494	20.515	20.548	20.606

Table 2 demonstrates that as the averaging interval increases, estimates of energy also increase, resulting in an overestimate of energy from hourly average weather of 0.6%. We next examined the energy produced on each of the 16 days, to elucidate the reasons for the overestimate of 0.6% for the aggregate energy.

Figure 7 shows energy (Wh) produced each day for three-second weather data, five minute averaged weather data, and for hourly-averaged weather, superimposed on a plot of the power for each day. For mostly clear days (i.e., Days 6, 8 and 9), energy estimated from three-second and five-minute average weather are approximately equal. However, energy is consistently underestimated using hourly average weather, by approximately 0.2%. In contrast, energy is overestimated on days with variable irradiance (e.g., Day 10), by increasing amounts as the averaging interval lengthens: at hourly averages, energy is overestimated by as much as 1.6%. For days exhibiting both clear and variables periods, e.g., Day 4 and Day 15, energy may be underestimated or overestimated. Error in calculated energy results from the approximation of

power in each interval $[t_k, t_{k+1}]$ by the representative value $P(t_k^*)$ in Eq. (8). Theory guarantees the existence of a value $P(t_k^*)$ which, if used, would result in zero error in the calculation of energy. However, in our calculations the representative values $P(t_k^*)$ are determined by using time-averaged weather and representative values for *AMa* and *AOI*. Thus, the causes for error in energy can be traced back to the calculation of power from time-averaged weather data.
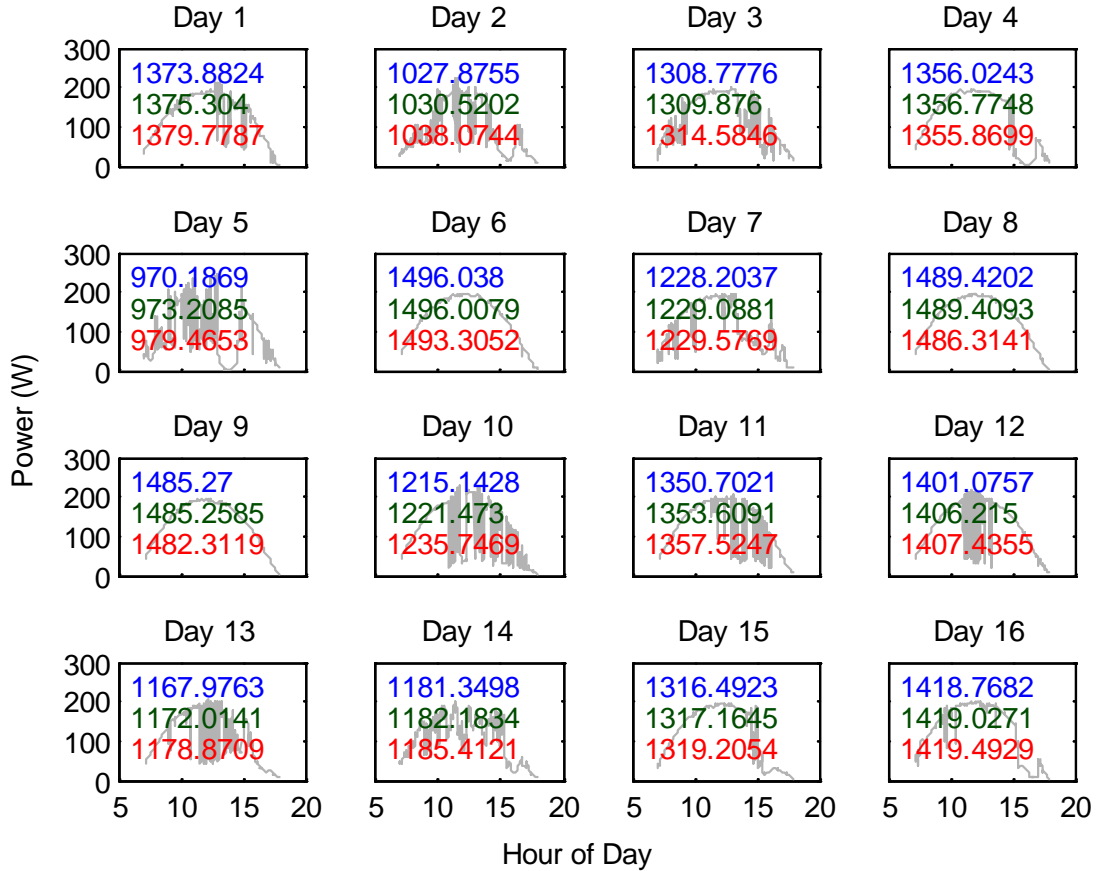
Figure 7. Energy by Day for a Y230 Module: Three Second Weather Intervals (blue), Five Minute Average (green) and Hourly Average Weather (red).

We next investigated the dependence of energy error on the time of day. When the error in energy is calculated for each hour, we observe that the error depends on the time of day and the variability in irradiance as well as on the averaging interval. To illustrate these dependencies, Figure 8 shows calculated power for 3 second and 60 minute averages of weather, and error in energy for each hour of the day, for 15 minute and 60 minute averages of weather. For a clear day (Figure 8, top row), the largest errors are underestimates of energy which occur early in the morning or late at night; during midday, errors are small. The pattern of energy errors for clear days illustrated in Figure 8 (top right plot) is typical: energy is underestimated for early or late hours that have relatively low but rapidly changing effective irradiance, whereas errors for

24

midday hours followed a shallow U shape. On a variable day (Figure 8, bottom row), the largest errors are overestimates of energy and occur at midday when irradiance is most variable.
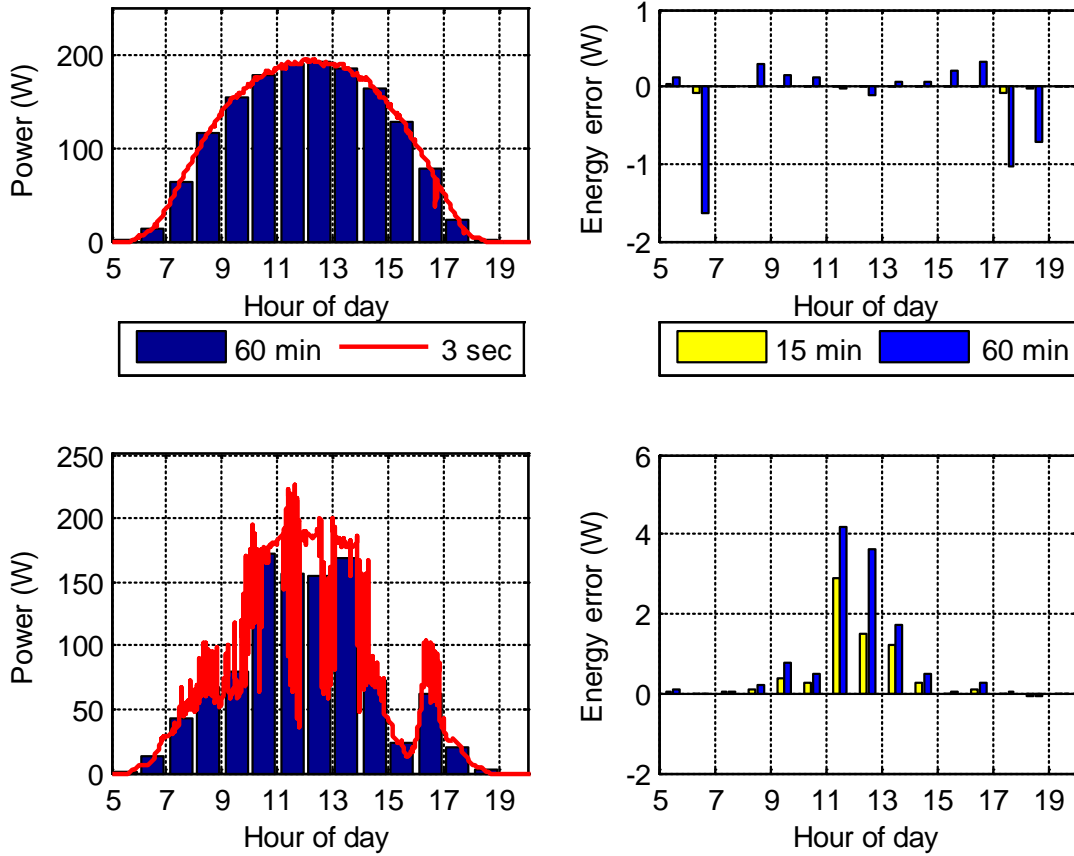
Figure 8. Power and Error in Energy for a Clear Day (Day 6; top) and a Variable Day (Day 2; bottom)

The errors illustrated by Figure 8 result from two different approximations:
1) the approximation of effective irradiance from time-averaged weather data and point values for *AMa* and *AOI*; and
2) the approximation of time-averaged power (i.e., $\overline{P}(E_e,\ldots)$) by the power computed from the time-averaged weather (i.e., $P(\overline{E_e},\ldots)$, see Figure 5).

Energy errors for clear days can be traced primarily to the first source, whereas energy errors for days with variable irradiance result from the combined effects of both sources.

Approximation of Effective Irradiance

Effective irradiance (E_e) is the solar radiation that is captured by the module's cells. For the Sandia Array Performance Model, effective irradiance is calculated in watts by ([1], Eq. 21):

$$E_e = E_e \left(E_b, E_{diff}, AMa, AOI \right)$$
$$= f_1 \left(AMa \right) \left(E_b f_2 \left(AOI \right) + f_d E_{diff} \right) \times SF \tag{10}$$

where

$f_1 \left(AMa \right)$ is the air mass (AMa) dependent spectral correction;

$f_2 \left(AOI \right)$ is the angle-of-incidence (AOI) correction;

E_b is the beam irradiance incident on the module;

E_{diff} is the diffuse irradiance incident on the module;

f_d is the fraction of diffuse irradiance captured by the module (typically set equal to 1);

SF is the soiling derate factor (set to 0.98 in this analysis).

E_b and E_{diff} are calculated from available irradiance measurements (e.g., direct normal irradiance or global horizontal irradiance) using various models (see [5] for a survey of methods.). AMa and AOI are typically calculated deterministically using only the solar position (ephemeris) [5].

As discussed in Sect. 2.2, as is common practice, we averaged E_b and E_{diff} over each time interval to obtain $\overline{E_b}$ and $\overline{E_{diff}}$, respectively, and we associated the values of AMa and AOI at each interval's midpoint, denoted by AMa^* and AOI^*, respectively, to the entire interval, with modification for intervals containing sunrise or sunset. We then calculated effective irradiance using Eq. (10) and obtained a single value $\hat{E}_e = E_e \left(\overline{E_b}, \overline{E_{diff}}, AMa^*, AOI^* \right)$ for each interval.

The value of $\hat{E}_e$ which results from time-averaged data is not equal to the average $\overline{E_e}$ of $E_e(\Delta t)$ over an interval because E_e is not linear with respect to the independent variables (Eq. (10)). We found that the error in energy for hours with clear sky conditions (e.g., between 6 am and 6 pm in Figure 8, top row) results almost entirely from the inexact approximation of $\overline{E_e}$ by $\hat{E}_e$. We confirmed this finding by recalculating power, using $\overline{E_e}$ over 60-minute intervals in place of $\hat{E}_e$ estimated from time-averaged weather data, and found that, when using the exact value of $\overline{E_e}$ in place of $\hat{E}_e$, the energy errors in each hour of a clear day were less than 0.001W. Consequently, we conclude that for clear days, the error in calculated energy is almost entirely attributable to the first source of error, the approximation of effective irradiance.

To illustrate the error in energy from the approximation of effective irradiance, we calculated the error in energy for each day of one year, using a clear-sky model for Albuquerque, NM, to estimate irradiance at one minute intervals, a constant ambient temperature of 25 °C, a constant wind speed of 1 m/s, and a single Y230 module fixed at latitude tilt. We calculated the error in energy for each hour of the year and normalized the error to each day's total energy. Figure 9

illustrates the reduction in error as the averaging interval is reduced. Depending on the time of year, the normalized absolute error using 5-minute intervals is generally (i.e., the 95th percentile of hourly errors for hours with energy) less than 0.034%, and is always less than 0.075%. For 15-minute intervals, the normalized absolute error is generally less than 0.031% and always less than 0.24%. For 60-minute intervals, however, the normalized absolute error is generally less than 0.3% but can be as great as 1.9%. Reducing the averaging interval from 60 minutes to 15 minutes reduces the normalized error by roughly a factor of 10.
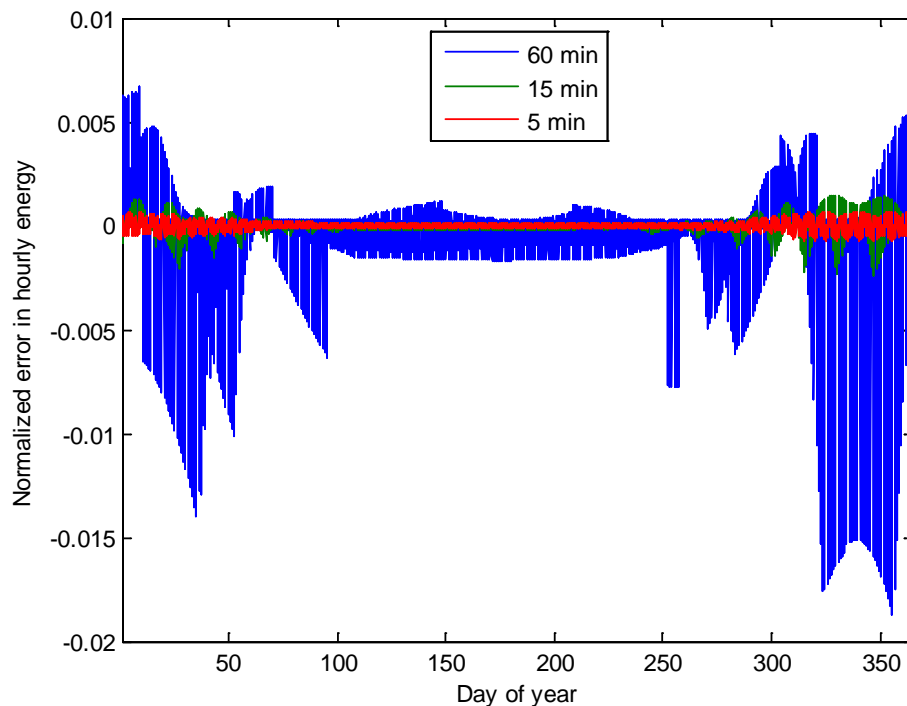
Figure 9. Error in Hourly Energy for One Year of Clear-Sky Days and Different Averaging Intervals: Albuquerque, NM.

We investigated the dependence of the error profile illustrated in Figure 9 on both location and technology. We anticipated that the error would vary significantly by location, due to changes in solar ephemeris, but not significantly for different technologies, because the response of any modules is nearly linear at low irradiance. We confirmed that the profile of this component of error varies significantly with longitude and latitude (Figure 10 shows the error profile for Lanai HI for the same Y230 module), and found some degree of variation, primarily in magnitude, by technology (Figure 11 illustrates the error profile for Lanai HI for a Cd-Te module at latitude tilt.)
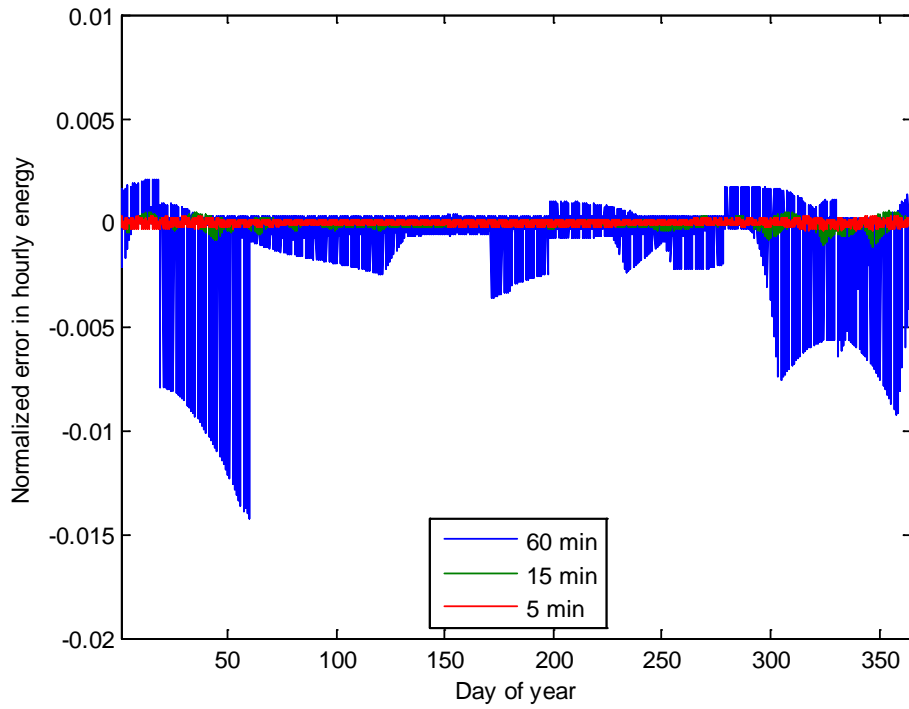
Figure 10. Error in Hourly Energy for One Year of Clear-Sky Days and Different Averaging Intervals: Y230 module at latitude tilt, Lanai, HI.
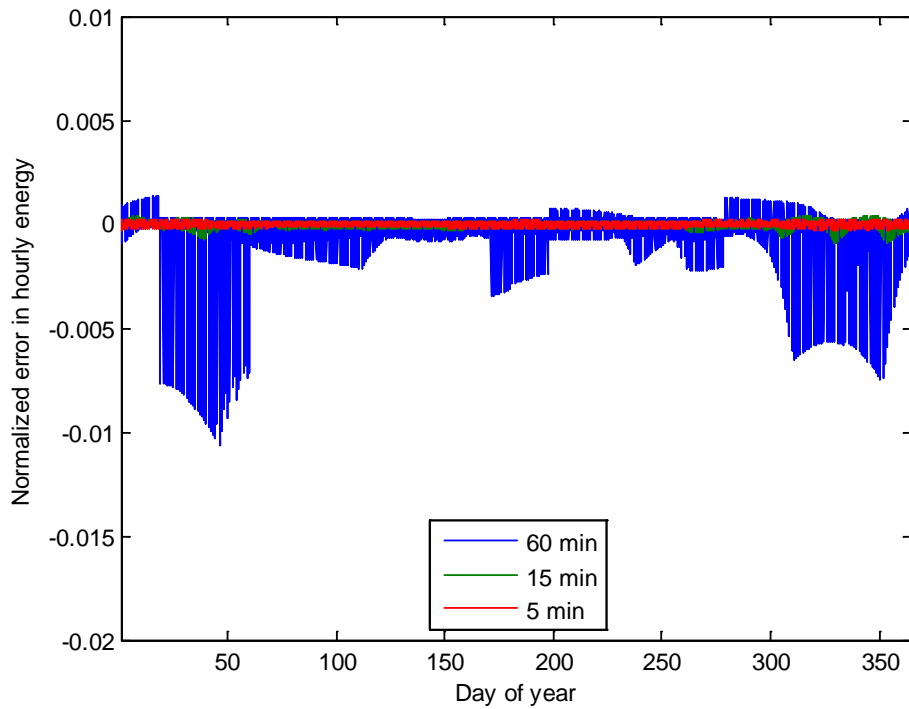
Figure 11. Error in Hourly Energy for One Year of Clear-Sky Days and Different Averaging Intervals: CdTe module at latitude tilt, Lanai, HI.

28

We explored methods to correct the error illustrated in Figure 9. The envelope of the error shown in Figure 9 is defined by the greatest positive and negative errors for successive days. To illustrate when these errors occur during each day, Figure 12 shows errors by hour for one day in the annual sequence depicted in Figure 9. The profile illustrated in Figure 12 is typical for many clear days: large errors in early and late hours, with a shallow 'U' shape in between. We note that the sign of the error changes in the two earliest hours. The sign and magnitude of the errors in early and late hours depends substantially on the interaction between the approximate values for averaged beam and diffuse irradiance (calculated here using the clear-sky model) and the selection of point values for *AMa* and *AOI* for these hours. The shape displayed in Figure 12 changes over different days throughout the year, as the sunrise and sunset times move through clock hours as indicated by the complex shape of the upper and lower edges of the error envelope displayed in Figure 9. Accordingly, although a correction factor could be developed for the day illustrated in Figure 12, different values would be required for different days. We conclude that it is unlikely that a simple correction factor could be developed and applied to counter the error in energy that results from approximating effective irradiance.
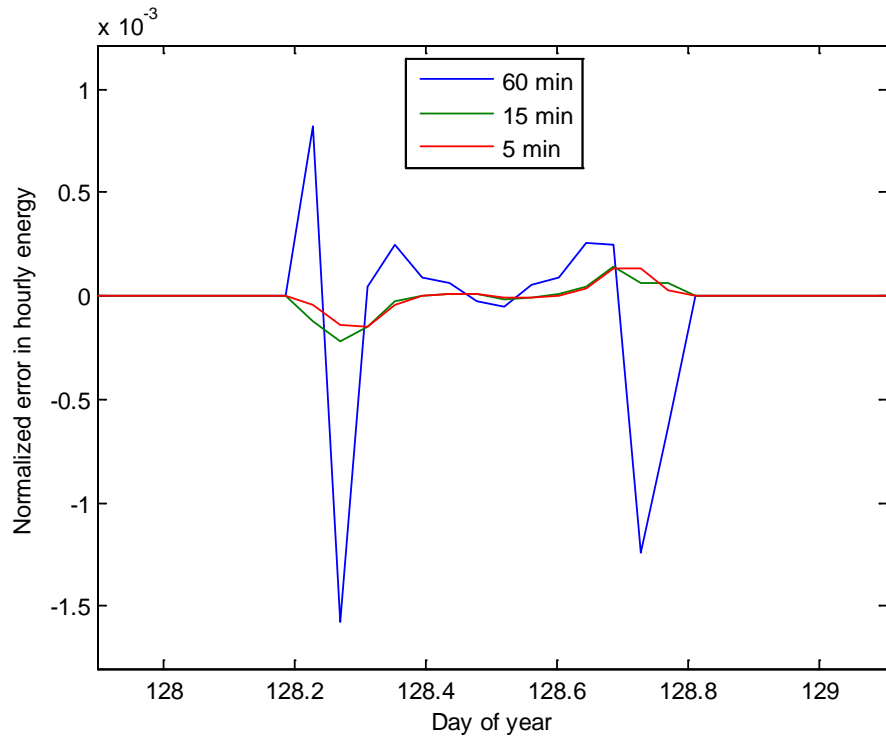
Figure 12. Error in Energy by Hour for One Clear Sky Day.

Because *AMa* and *AOI* are calculated deterministically without measurement, we explored combining exact values for *AMa* and *AOI* at one-minute resolution with the available values for E_b and E_{diff}, i.e., by applying $\overline{E_b}$ and $\overline{E_{diff}}$ to each minute in the hour. We found little reduction in the energy error indicating that increasing precision in the values for *AMa* and *AOI* alone would not correct the error in calculated energy. More precise value for $\overline{E_b}$ and

$\overline{E_{diff}}$ can only be obtained by more frequent irradiance measurements. We conclude, therefore, that error in energy calculations resulting from approximation of effective irradiance by time-averaged quantities best reduced by increasing the frequency of irradiance measurements.

Approximation of Time-Averaged Power

Power calculated from time-averaged weather data (i.e., $P\left(\overline{E_e},\ldots\right)$) is an approximation to the time-average of power (i.e., $\overline{P}\left(E_e,\ldots\right)$) that is calculated from weather data at each time step. Figure 5 illustrates how this approximation can be in error due to the curvature in the module's response to effective irradiance. Because of the downward curvature in the module's response, $P\left(\overline{E_e},\ldots\right)$ tends to be an overestimate of $\overline{P}\left(E_e,\ldots\right)$.

During midday hours with clear sky conditions (e.g., between 11 am and 2 pm on Figure 8, top row), the error in energy arising from the approximation of time-averaged power is relatively small because there is little variability in irradiance. Each irradiance measurement in a time interval is similar to the average irradiance over the interval; thus power computed from the time-average of irradiance is similar to the time-average of power. However, when irradiance is variable within the time interval (e.g., between 11 am and 2 pm on Figure 8, bottom row), time-averaged power (and hence energy) are overestimated from time-averaged weather. Error magnitude decreases with decreasing averaging interval.

For clear-sky periods, the error in energy resulting from the approximation of time-averaged power is small relative to the error in energy from the approximation of effective irradiance (e.g., Figure 12). For periods with variable irradiance, the error in energy from the approximation of time-averaged power can be greater than the error from the approximation of effective irradiance. To illustrate, we calculated power at one-minute intervals (for a latitude tilt Y230 module) using weather recorded during 20 days of April, 2010 at Lanai, HI (Figure 13). Irradiance exhibited large and rapid variations during many hours of the recorded weather data. These variations, which translate directly to variations in power at three-second intervals, are smoothed somewhat in the power calculated using weather averaged over five-minute intervals, and are largely obscured in the power calculated from hourly average weather.

Figure 14 illustrates the relative error in hourly energy (i.e., energy for each hour normalized by the total daily energy) for the twenty days of weather from Lanai, HI. We note that during the period of time selected, the approximation of effective irradiance introduces relatively large negative errors in energy at late hours; this component of error is most visible during clear afternoons (e.g., Day 11) or afternoons during which irradiance variability was small in magnitude (e.g., Day 14, 15 or 16). During the middle periods of many days, averaging tends to overestimate energy, as predicted from consideration of Figure 5, with the relative error increasing as the averaging interval lengthens. However, the magnitude of the relative error varies in a complex manner between days, and it appears unlikely that a correction factor could be estimated from considering the variability in irradiance and the average hourly irradiance. For example, during the middle of both Day 4 and Day 9, irradiance is highly variable around moderate values for the hourly average irradiance. However, the relative errors on these two

days are quite different, and shown in Figure 14. Moreover, similar errors are observed for a day with highly variable irradiance (Day 7) as for a day with somewhat variable irradiance (Day 2). Consequently, we conclude that error in energy calculations resulting from approximating time-averaged power by power calculated from time-averaged weather quantities is unlikely to be reduced without reducing the time-averaging interval.
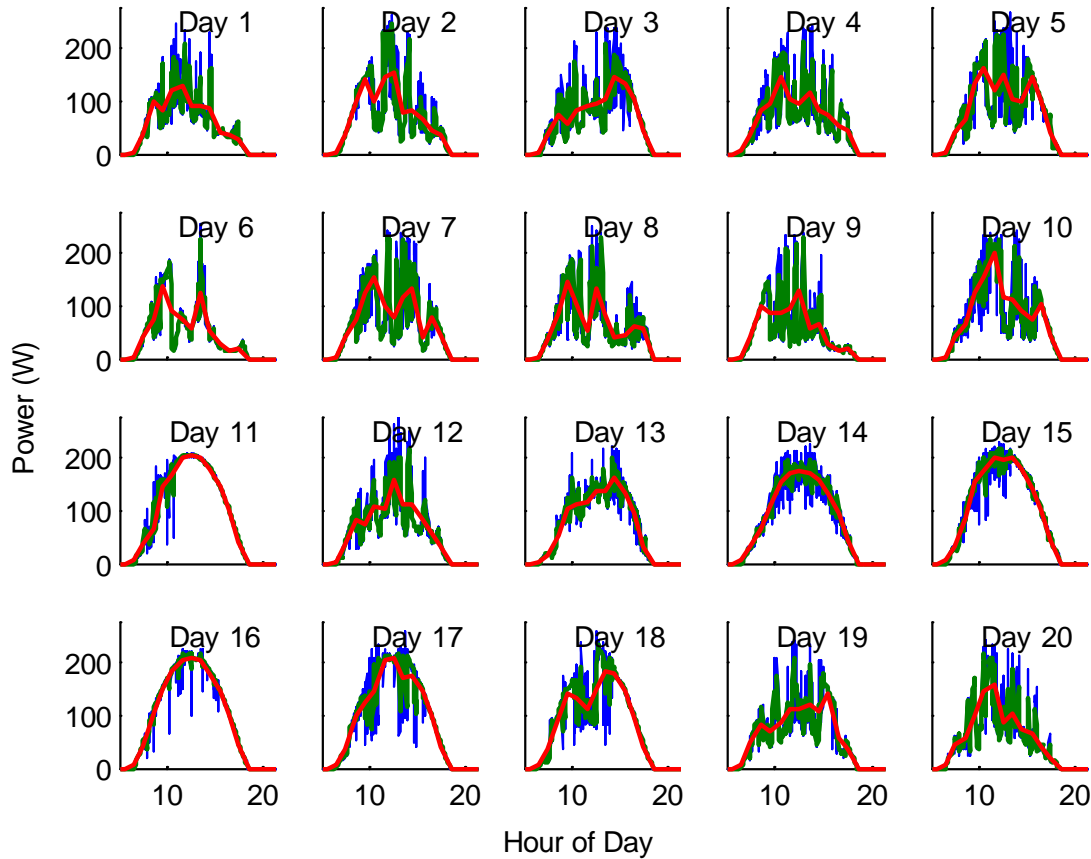
Figure 13. Estimated Power for Lanai, HI: One Minute Weather Intervals (blue), Five Minute Average (green) and Hourly Average Weather (red).
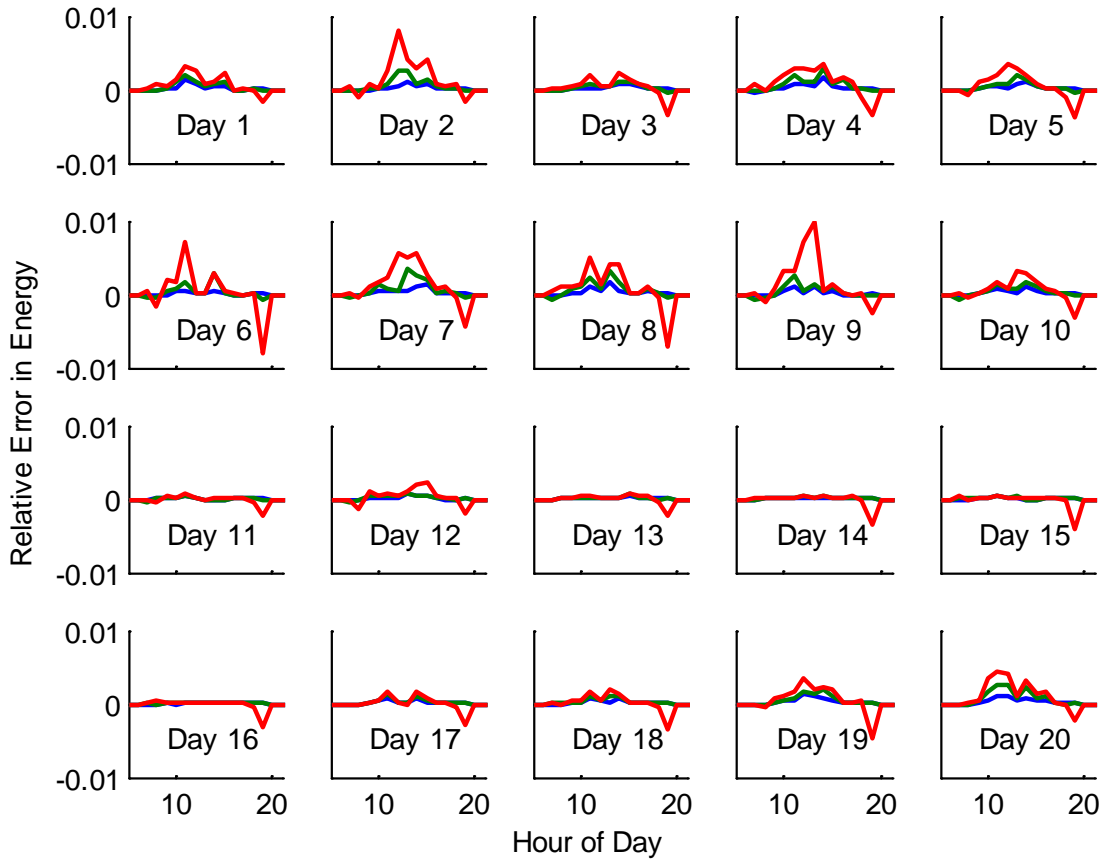
Figure 14. Relative Error in Hourly Energy for Lanai, HI: Power Calculated From Five Minute Average (blue), Fifteen Minute Average (green) and Hourly Average Weather (red).

2.4.3. Effect of Averaging on Aggregate Annual Energy

The discussion in the preceding section shows that the error in daily energy can be either positive or negative at different times during the year. To determine whether positive and negative errors during the year offset sufficiently to yield an accurate estimate of annual energy, we calculated the error in aggregate annual energy, for various locations, using both actual and modeled weather. Results are summarized in Table 3.

For the representative location with consistently variable irradiance (Lanai, HI), we calculated energy for a single latitude tilt Y230 cSi module using measured DNI, diffuse irradiance, ambient temperature and wind speed from the NREL MIDC station for 2010 [13]. We observe that the error in annual energy is positive (i.e., energy is overestimated) for all averaging intervals, consistent with the preceding analysis indicating that aggregate energy is anticipated to be overestimated during variable irradiance conditions. For the representative location with frequent clear sky irradiance conditions (Las Vegas, NV), we calculated annual energy for the

same PV module using measured DNI, diffuse irradiance, ambient temperature and wind speed from the NREL MIDC station at the University of Nevada, Las Vegas for 2010. We found that the error in annual energy is positive but remains relatively small for all averaging intervals. The decrease in relative error from 0.09% to 0.04% when the averaging interval increases from fifteen minutes to one hour results because the effects of the two approximations are not commensurate as the averaging interval increases. As the interval lengthens, the component of error due to the approximation of effective irradiance decreases rapidly (i.e., favors underestimating energy), whereas the component of error due to the approximation of time-averaged power increases (i.e., favors overestimating energy) but more slowly. The net error in energy when both components are combined remains positive for the Las Vegas data.

Table 3. Error in Annual Energy for Various Locations and Averaging Intervals.

| Location | Irradiance conditions | Error (%) in annual energy for each averaging interval | | |
		5 min.	15 min.	1 hr
Lanai, HI (2010)	Consistently variable throughout the year	0.3	0.6	0.8
Las Vegas, NV (2010)	Many clear days with infrequent cloudy periods	0.03	0.09	0.04
Lanai, HI (clear sky model)	Completely clear (modeled)	–0.003	–0.01	–0.3
Albuquerque, NM (clear sky model)	Completely clear (modeled)	–0.002	–0.007	–0.3

To obtain a lower bound on error in annual energy due to time averaging, we also calculated annual energy for one year using a clear sky model, for both Lanai, HI and Albuquerque, NM. We observe that errors are similar for both locations.

We conclude that error in annual energy for a single latitude tilt Y230 cSi module estimated using hourly averaged weather ranges from an upper bound of roughly 1% (i.e., energy is overestimated) for locations with consistent, highly variable irradiance conditions, down to -0.3% (i.e., energy is underestimated) for locations with persistent clear sky irradiance conditions. Error annual energy for a range of module technologies is addressed in Section 2.4.5.

2.4.4. Potential Correction of Errors in Energy

Error in calculated energy results from the combined effects of the two approximations discussed in Section 2.4.2. In combination over a period of time, errors from the approximations may be offsetting: for example, the underestimate of energy for some time intervals due to the approximation of effective irradiance may be offset by the overestimate of energy for other time intervals with variable effective irradiance. We explored the extent to which the aggregate error in energy might be predicted from module characteristics, and possibly corrected absent additional weather measurements. For a selected sample of PV modules for which the Sandia Array Performance Model has been calibrated, we computed power and energy and examined the dependence of the error in energy on module technology, the curvature in the module's

response to effective irradiance in the outdoor environment, and the averaging interval applied to the weather data. We performed our analysis using weather data for three locations with different climates:

- Albuquerque, NM, 16 days in late August and early September 2008 (mix of clear and cloudy days), using data obtained by Sandia National Laboratories;
- Las Vegas, NV, 30 days in August 2008 (many clear days), using data obtained from the Las Vegas Valley Water District at the Las Vegas Springs Preserve;
- Lanai, HI, 20 days in April 2010 (most days are cloudy), using data obtained by Sandia National Laboratories.

We also calculated power and energy for each module for one year of clear-sky irradiance estimated by a clear-sky model for Albuquerque, NM.

We quantified the curvature in a module's response to effective irradiance by calculating the vertical distance from the average of power at $E_e = 1000$ W/m^2 (average calculated for effective irradiance between 997 W/m^2 and 1002 W/m^2) and a line fit to power for $0 \leq E_e \leq 400$ W/m^2 (Figure 15). For this calculation, we used irradiance, temperature and wind speed for Albuquerque, NM; similar values would be obtained at other locations. We chose to measure curvature in this manner because, for many technologies, module response to effective irradiance is essentially linear at low irradiance, and the error in energy that depends on the curvature in a module's response is larger at higher irradiance. Table 4 lists the technologies represented in our selected sample of PV modules and the measure of curvature in each module's response. The lower values of curvature for the Cd-Te modules may be due to the lower temperature coefficients associated with this cell material. The higher curvature for 3-a-Si modules is likely due to the combined effects of higher power performance at low irradiance (compared to single

Table 4. Module Technologies Selected for Analysis of Energy Error

Index	Technology Type[1]	Curvature (fraction of max. power)	Index	Technology Type[1]	Curvature (fraction of max. power)
1	3-a-Si	0.197	14	c-Si	0.071
2	3-a-Si	0.201	15	EFG mc-Si	0.069
3	CdTe	0.069	16	EFG mc-Si	0.045
4	CdTe	0.017	17	HIT-Si	0.043
5	CIS	0.004	18	HIT-Si	0.057
6	c-Si	0.152	19	HIT-Si	0.094
7	c-Si	0.080	20	mc-Si	0.099
8	c-Si	0.100	21	mc-Si	0.124
9	c-Si	0.092	22	mc-Si	0.082
10	c-Si	0.154	23	mc-Si	0.105
11	c-Si	0.103	24	mc-Si	0.121
12	c-Si	0.067	25	mc-Si	0.127
13	c-Si	0.075			

[1] 3-a-Si: triple junction amorphous silicon; CdTe: cadmium-telluride; CIS: Cu-In-Se; c-Si: crystalline silicon; EFG mc-Si: Edge-defined Film-fed Growth monocrystalline silicon; HIT-Si: Heterojunction with Intrinsic Thin-layer silicon; mc-Si: monocrystalline silicon.

junction technology) and the potential for additional electrical losses within the cell at high irradiance (again compared to single junction cells). We note that higher (or lower) values of this curvature metric do not imply better (or worse performance) than modules with different values; the metric only serves to quantify the degree of nonlinearity in the module's power vs. irradiance curve.
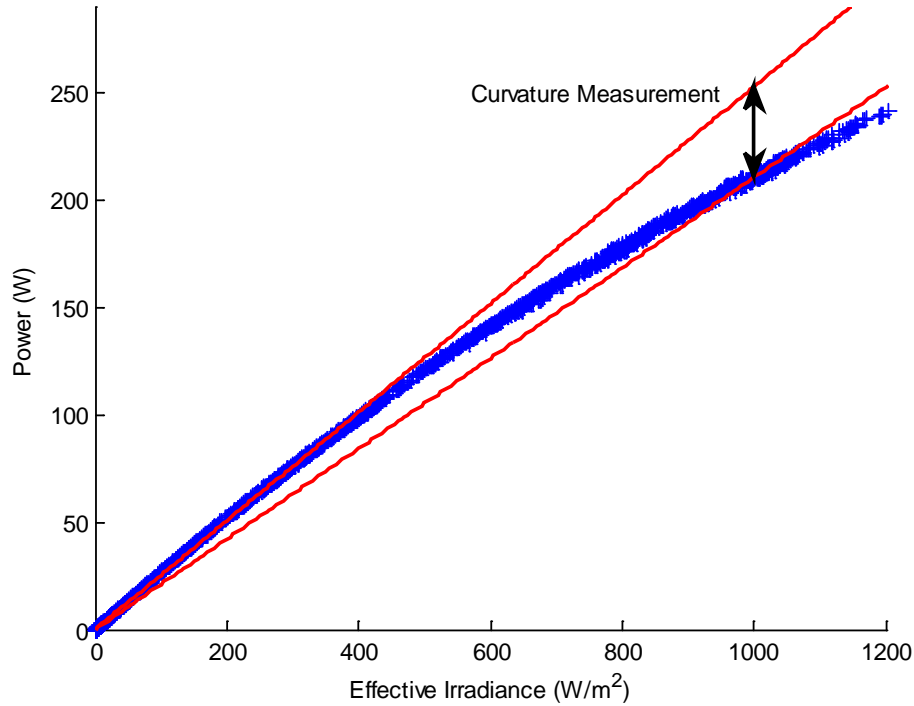
Figure 15. Illustration of Curvature Measurement for a Notional Module

For the weather in Albuquerque, we found that the average daily error in total energy (total error in energy over all days divided by number of days) for the time period considered (16 days in August/September, 2010) could be reasonably approximated as a linear function of the measure of module curvature (Figure 16). Moreover, for averaging intervals up to 15 minutes, the slopes and intercepts of the line increased regularly. However, for a 60-minute averaging interval, the data exhibit curvature and the intercept of the fitted line does not follow the trend shown for shorter averaging intervals.

For weather from other locations (i.e., Lanai, HI and Las Vegas, NV), we also found that average error in energy was generally linear with the module curvature measure, and that the slopes and intercepts of the fitted lines increased as the averaging interval increased (Figure 17). However, we observed that the parameters for the fitted lines depended strongly on location. In particular, in Las Vegas, NV, where the selected period included mostly clear days, both slopes and intercepts were less than observed for Albuquerque. In contrast, the selected period for Lanai, HI involved mostly days with variable irradiance, and the fitted lines showed greater slopes and intercepts.

To elucidate the reasons why error in energy varies between locations, we examined in detail the dependence of the error on clear sky or variable irradiance conditions. For Albuquerque, NM, Figure 18 shows the average daily error in energy as a function of the measure of module curvature; it is clear that the error for each day depends strongly on the variability of irradiance during the day (compare Figure 18 with Figure 2). In particular, on a clear day (e.g., Day 6) the error is relatively insensitive to module curvature. Given the dependence of error on irradiance conditions, and the dependence of error for clear-sky conditions on the time of year (Figure 9), it is not reasonable to expect to obtain a simple model for aggregate energy error as a function of module curvature. However, we speculate that, if the approximation of effective irradiance was improved such that its contribution to energy error is greatly reduced, then it may be possible to obtain an effective correction for aggregate energy error as a function of module curvature and a measure of the fraction of hours with clear-sky conditions.
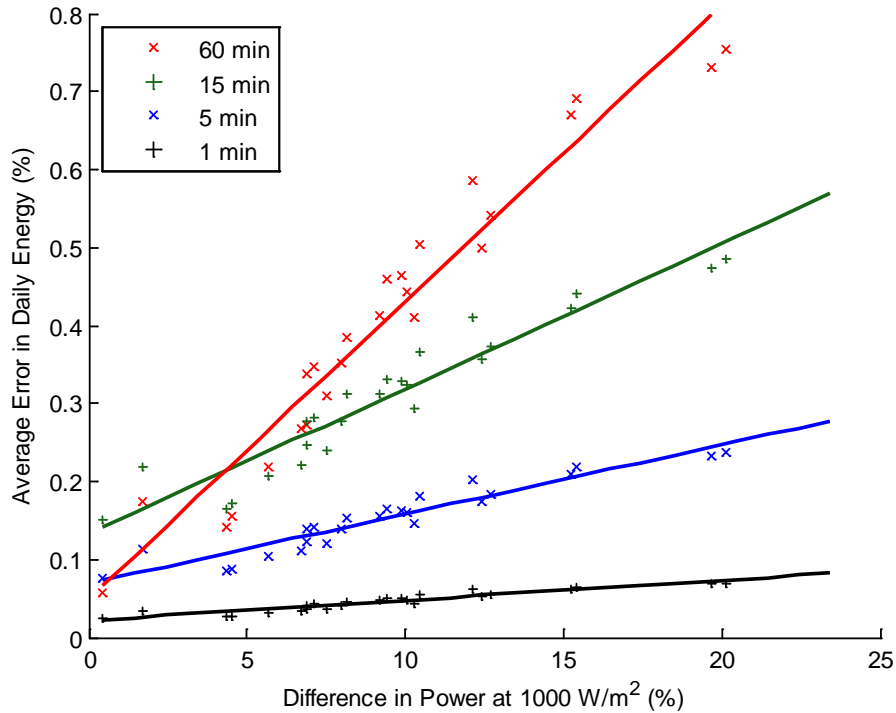
Figure 16. Average Error in Daily Energy as a Function of Module Curvature: Fall Weather in Albuquerque, NM
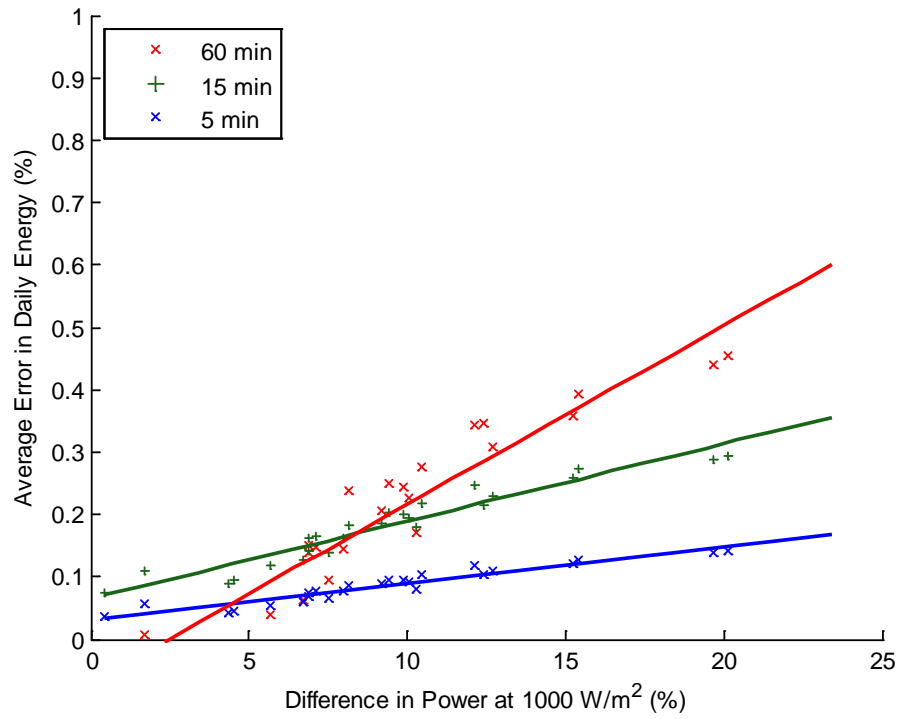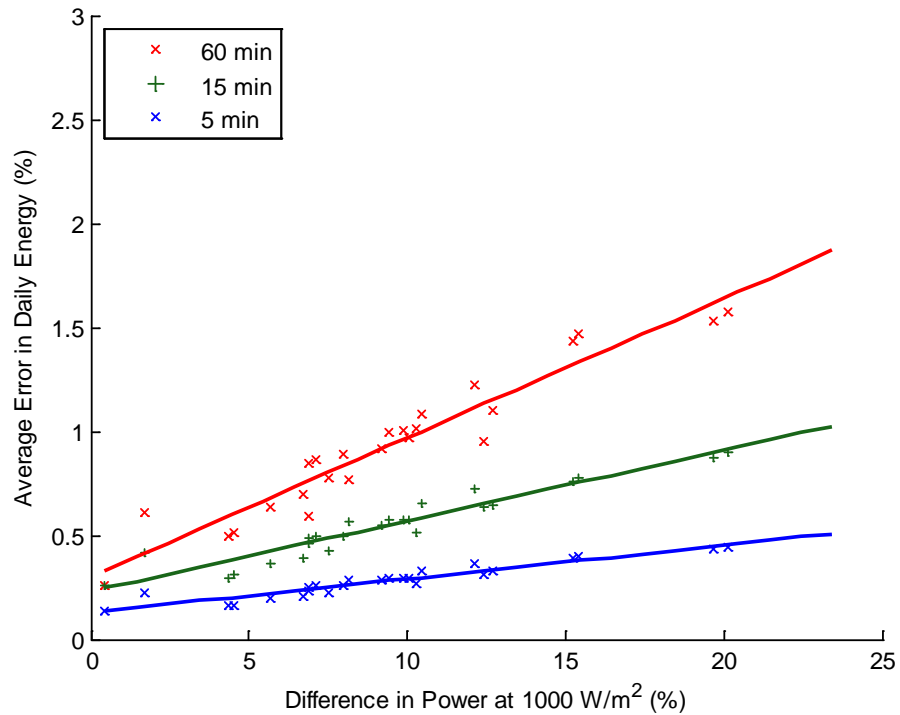
Figure 17. Average Error in Daily Energy as a Function of Module Curvature: (a) Spring Weather in Las Vegas, NV, and (b) Spring Weather in Lanai, HI.
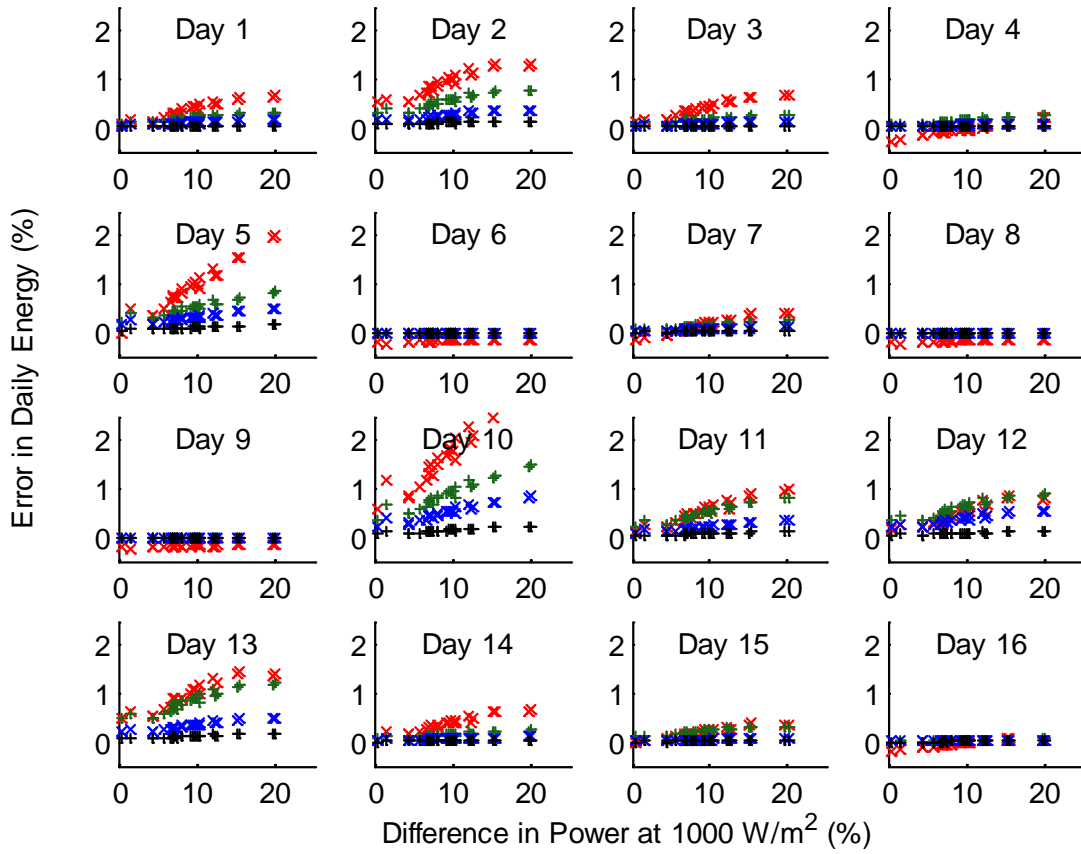
Figure 18. Error in Energy for Each Day as a Function of Module Curvature in Albuquerque, NM: 1 Minute (black), 5 Minute (blue), 15 Minute (green) and 60 Minute Averaging Intervals (red).

2.4.5. Dependence of Annual Energy Error on Module Technology

Because one component of error in energy arises from the curvature in a module's response to increasing irradiance (illustrated in Figure 15), the error in annual energy is dependent the combination of module technology, irradiance variability and time scale for averaging. We calculated the error in annual energy, for various locations, using both actual and modeled weather, for three modules representing the range of observed curvature values: the least (1.7%, index 4 in Table 4); 9.6% for the representative Yingli Y230 cSi module; and the greatest (20.1%, index 2 in Table 4). Results are summarized in Table 5.

Error in annual energy generally increases as module curvature, variability in irradiance and averaging interval increase. Error may be either positive when variable irradiance conditions dominate, or negative when clear sky conditions dominate. Increasing module power curvature amplifies the error during variable irradiance periods, whereas increasing the averaging interval amplifies the error during any irradiance conditions. The values given in Table 5 permit us to

offer a range of error in energy calculations resulting from time-averaged weather, from -0.3% for modules with little power curvature in persistently clear conditions, to 2% for modules with significant power curvature in consistently variable irradiance conditions.

Table 5. Error (%) in Annual Energy for Various Module Technologies, Locations and Averaging Intervals.

Location: Irradiance condition	Averaging Interval (minutes)	Curvature (fraction of power at 1000 W/m²)		
		1.7%	9.6%	20.1%
Lanai, HI (2010): Consistently variable throughout the year	5	0.17	0.3	0.36
	15	0.28	0.6	0.61
	60	0.37	0.8	1.8
Las Vegas, NV (2010): Many clear days with infrequent cloudy periods	5	0.02	0.03	0.06
	15	0.04	0.09	0.17
	60	–0.04	0.04	0.34
Lanai, HI (clear sky model): Completely clear	5	–0.002	–0.003	–0.003
	15	–0.012	–0.01	–0.014
	60	–0.23	–0.3	–0.19
Albuquerque, NM (clear sky model): Completely clear	5	–0.003	–0.002	–0.002
	15	–0.011	–0.007	–0.022
	60	–0.25	–0.3	–0.18

2.6. Implications for PV System Design

Design of a PV system includes selection of components, including the modules and inverters, and is typically supported by modeling of the proposed system to estimate the power and energy output. Often, only hourly weather data is available for use in the performance models, and system design decisions do not currently take into account the error in estimated power and energy resulting from the use of hourly-averaged weather data.

For example, it is common practice to estimate the DC power output of the modules using a performance model, and to use the range of the DC power output and the total projected energy to guide selection of an appropriate inverter. Other authors have commented on the potential loss of energy from the system when the inverter is sized to saturate at less than the maximum DC power, and have observed that the loss of energy is compounded when maximum DC power is estimated from time-averaged weather data. Ransome and Funtan [14] compared the total AC yield (kW/kWp) for several module technologies calculated using irradiance and module temperature measured at 15-second intervals. They include a day with variable irradiance in their analysis; during variable conditions irradiance may briefly exceed clear sky values due to cloud enhancement [15]. Their results illustrate the potential for AC power to be curtailed by the inverter if the inverter is sized to saturate at 90% of the DC power rating of the PV module. They do not calculate a probability of curtailment, nor estimate the reduction in total energy over a period of time resulting from curtailment. In addition, their analysis did not account for the

numerical error in the estimated maximum DC power which results from the use of time-averaged weather data.

Use of time-averaged weather data underestimates maximum power due to the reduction in irradiance variability (Section 2.3.2) and thus may lead to selection of a smaller inverter than would be selected if higher resolution weather data were used. In addition, unless weather is persistently clear, the energy projected by models using time-averaged weather data is likely to be overstated to some degree (Section 2.4.2). These two effects on inverter size selection are compounding, and both must be considered when determining the marginal value of increasing the inverter size.

Figure 19 illustrates these combined effects. A performance model can be used to calculate energy as a function of inverter size using hourly-averaged weather to obtain the notional blue curve in Figure 19. In Figure 9Figure 19, the "notional inverter size" is the ratio of the AC rating of the inverter and the DC (STC) rating of the PV array. Energy increases with inverter size until the inverter becomes large enough to capture all the modeled power. Assume that an inverter size is selected on the basis of this calculation, perhaps by considering the marginal cost of increasing the inverter size as compared to the marginal gain in estimated energy.

Using the same inverter, system performance can also be calculated by supplying weather at high time resolution. Because the inverter size was selected from analysis using hourly average weather that is less variable than high resolution weather, we expect that the inverter will limit AC power during short intervals where module DC power is greater than in the hourly average analysis. Thus simulation of the system with the high resolution weather data will project *less* energy than when hourly-averaged weather is used. The reduction results because the inverter prevents the model from accumulating energy (i.e., the inverter clips power) during the short periods of time when module DC power exceeds the inverter saturation limit. Consequently, the high-time resolution results, illustrated in Figure 19 by the green curve, are drawn below the blue curve.

Because the green curve is a more accurate representation of projected energy, the value of increasing the inverter size should be quantified by this curve, rather than by the blue curve. It seems difficult (if not impossible) to find a method to correct the blue curve so as to obtain an accurate estimate of the value of a larger inverter using hourly average weather. The blue curve is subject to error due to the use of time-averaged data, as discussed in Section 2.4, and likely represents an overestimate of energy from the system. Correcting the overestimate would shift the blue curve downward to one of the two displayed red curves. If the error in energy due to time averaging exceeds the energy foregone due to inverter clipping, the shift downward may be greater than the difference between the blue curve and the green curve. However, accurate calculation of the red curve would require a method of correcting the error in energy from using hourly-averaged weather, which we concluded is difficult to accomplish (Section 2.4.2). The most effective method to preclude error from affecting choice of the inverter size is to use weather data at shorter time intervals.
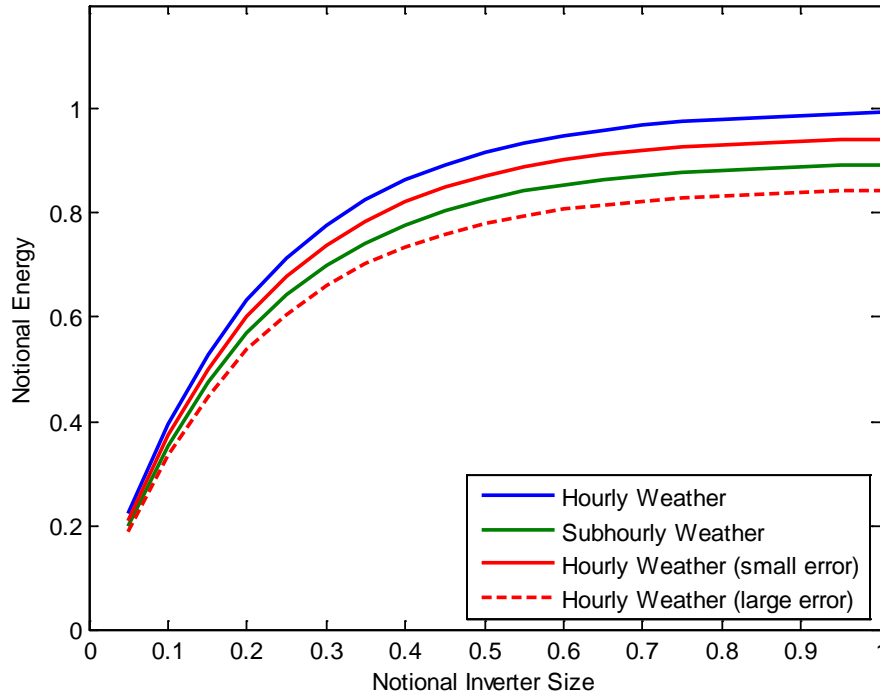
Figure 19. Illustration of Effects on Inverter Size.

The same conclusion was reached in [16], where the authors examined the effect of inverter saturation on annual energy. Using one-second irradiance measurements and an inverter sized as a fraction of the PV system DC rating, Luoma et al [16] quantify the loss in annual energy for a PV system located near San Diego, CA. They also estimate annual energy using time-averaged weather; comparison of annual energy among the various time-scales revealed that accurate estimate of the energy loss due to inverter saturation is only possible for calculations performed at short time scales.

2.6. Power Quality on a Grid with Connected PV

Time series of power from PV systems are used with grid simulation tools to calculated anticipated voltage levels on feeder circuits with connected PV. Voltage levels, and changes in voltage levels, form the basis for studies of the effects of grid-connected PV on the quality and stability of power. These studies examine effects that span a wide range of time scales:

- Net demand and production on circuits with connected PV systems. These studies essentially determine the energy balance at each point in time as the difference between load and PV power. Time scales used can range from hours to seconds, depending on the objectives of the particular study.
- Effects on automatic voltage control equipment (e.g., regulators and capacitors). These studies typically estimate the ability of the equipment to maintain steady-state voltage within tolerances, and the increased use of switches and taps, in response to variations in

grid-connected PV output and in load. For these studies, PV output data are at approximately one-minute or shorter time scales.

- Effects of rapid changes in PV power on voltage (i.e., flicker). Rapid and repeated deviations from steady-state voltage may cause unacceptable "flicker" in the power delivered to loads (e.g., lights). Simulations to assess the potential for flicker typically use a time interval of one second or less.

Estimating net demand and production conceptually amounts to comparing load and generation (including PV system power) at each point in time. The effects of time scale on estimated PV system power are discussed in Section 2.3. Widén et al. [17] examined the results of comparing time-averaged loads with time-averaged PV system power for ten-minute and hourly averages, and showed that the differences between the two averages narrow as the time-averaging window increases. They caution that imports and exports of power from the distribution system may be underestimated at longer averaging times, but do not conclude that any particular averaging time is sufficiently short to ameliorate the concern.

Because the time scales for power quality studies are similar to the finest time scales for measuring irradiance (and hence for estimating power from PV systems), little has been published regarding the effects of time scales for PV power data on power quality studies. Widén et al. [17] compared measured voltage levels at a residence with a PV system that is allowed to deliver excess power to the grid. They examined the distributions of steady-state voltage levels for ten-minute and hourly averaged voltage measurements, and concluded that the fraction of time spent at each voltage is similar for these two time averaging intervals. For studies of voltage stability where ten-minute time scales are informative, they conclude that hourly average measurements are sufficient. They do not explore the distribution of voltage levels at finer time scales.

Studies of power balance on a grid with connected PV systems will be subject to the errors described for power (Section 2.3) if the PV system power is estimated from weather averaged over long time scales. However, it seems reasonable to view these errors (which are on the order of 1%) as small in comparison to likely errors or variability in other quantities necessary for such analyses, such as load on the grid.

If irradiance (and other weather variables) are measured at times scales comparable to those relevant for power quality studies, i.e., at one second or less, then it seems unlikely that weather variables would be averaged over time intervals long enough to present a concern about introducing error. The important question, however, is whether the models that translate weather to PV power are appropriate. Most power models represent the system in its steady-state condition, and do not represent transients in power from, for example, thermal gradients across PV modules and arrays or capacitive charging or discharging.

3. CONCLUSIONS

We used common modeling practices to calculate PV module performance with the Sandia Array Performance Model for various locations and for weather data averaged over time intervals ranging from three seconds to one hour. We compared results calculated at different averaging intervals to examine the effect of time-averaging on the distribution of power, variability in power, and energy from the PV system.

We found that, in general, average power is overestimated, the distribution of power is narrowed, and variability in power is understated when power is calculated from time-averaged weather (Section 2.3). The overestimate of average power results from the nonlinear response of PV modules to changes in irradiance. For a typical cSi module, the overestimate of average power is on the order of 1% at hourly-averaged weather (see Table 1); the overestimate would be greater for multi-junction amorphous silicon modules, and less for CdTe modules (Table 5). The distribution of power is narrowed because averaging weather removes extreme values of irradiance and temperature. For weather recorded in Albuquerque, NM, the standard deviation of power is reduced by 10% and the 99th percentile by 7% when power is calculated from hourly averaged weather. If accurate calculation of statistics for power is desired, we recommend that weather measurements have a time interval of 5 min or less, to reduce error in the estimated percentiles of the distribution of power.

We observed that the rates of changes in power (i.e., ramp rates) are reduced in results calculated from time-averaged weather. The reduction in largest ramp rates can be substantial (Figure 6). Consequently care should be taken to select a time scale for weather data that is consistent with and appropriate for a study's objectives.

We also found that energy calculated from time-averaged weather is subject to error that increases as the averaging interval lengthens (Section 2.4). At hourly intervals, error in energy ranges from -0.3% to 2% (Table 5). The approximation of effective irradiance which results from using time-averaged weather measurements tends to underestimate energy, whereas the nonlinearities in the PV module's response to irradiance and associated environmental conditions contributes to overestimation of energy. The analysis showed that annual energy may be underestimated for locations with predominately clear sky irradiance conditions, by as much as 0.3% for hourly averaged weather, for most module technologies. In contrast, when hourly-averaged weather is used for locations with consistently variable irradiance conditions, annual energy from modules that are significantly nonlinear may be overestimated by as much as 2%. The aggregate error in annual energy resulting from the use of hourly averaged weather for any location is expected to fall within this range, i.e., between -0.3% and 2%, with values increasing as the frequency of variable (i.e., partly cloudy) irradiance conditions increases and with greater overestimates possible for modules with stronger nonlinear response.

We explored the feasibility of developing corrections for this error. Because the error in energy depends in a complex manner on the PV system's location and the module's characteristics, we concluded that development of an error correction method would be quite challenging and would depend on time, geographic location, PV technology, and seasonality. Therefore, such a correction was not attempted.

However, we observed that the errors in energy are significantly reduced when the time interval between weather measurements is shortened. For example, reducing the weather interval from one hour to 15 minutes generally reduces the error in energy by a factor of 10. Moreover, error is reduced as the module's response to changes in irradiance becomes more linear (i.e., the curvature illustrated in Figure 15 decreases). For a PV system and location, analysts may estimate the potential error in energy calculations arising for various time-averaging intervals by using a performance model and representative weather (i.e., concurrent irradiance and temperature) to estimate the curvature in the module's response to irradiance; then using Table 5 as a guide to possible errors. For modules with linear response to irradiance, longer time-averages of weather may be acceptable, whereas for modules with significantly non-linearly behavior, shorter averaging intervals may be necessary.

We considered the effects of error in energy on the selection of an inverter size for a PV system. Intuition suggests that that selecting inverter size based on analysis with hourly-averaged weather would lead to smaller inverters, because hourly averaging removes extreme values of irradiance and hence of power. A smaller inverter would limit power during these periods of peak irradiance and hence forego energy. This study originally intended to quantify the lost energy and its dependence on the averaging interval for weather used in system analyses. However, our analysis showed that it is difficult to untangle and separately correct for the comingled effects of using time-averaged weather: the overstatement of mean power; the narrowing of the distribution of power; and the errors which affect estimated energy. Consequently, if it is desired to eliminate the effect of these errors on the design of a PV system, the most effective method appears to be to use shorter time intervals for weather data, on the order of 15 minutes or less.

4. REFERENCES

1. D. King, W. Boyson, and J. Kratochvil, *Photovoltaic Array Performance Model*, SAND2004-3535, Sandia National Laboratories, Albuquerque, NM, December 2004.
2. W. De Soto, S. A. Klein, and W. A. Beckman, *Improvement and validation of a model for photovoltaic array performance*, Solar Energy, Vol. 80, pp. 78-88, 2006.
3. http://www.nrel.gov/rredc/pvwatts/
4. André Mermoud, Thibault Lejeune, *Performance Assessment of a Simulation Model for PV Modules of Any Available Technology*, Proceedings of the 25th European Phtovoltaic Solar Energy Conference, Valencia Spain, September 2010.
5. Eduardo Lorenzo, *Energy Collected and Delivered by PV* Modules, in Handbook of Photovoltaic Science and Engineering 2ed, ed. A. Luque and S. Hegedus, Wiley, 2011.
6. David L. King, Private communication, December, 2011.
7. Thomas L. Stoffel and Daryl R. Myers, *Accuracy of Silicon versus Thermopile Radiometers for Daily and Monthly Integrated Total Hemispheric Solar Radiation*, in Reliability of Photovoltaic Cells, Modules, Components, and Systems III, Ed. Neelkanth G. Dhere, John H. Wohlgemuth, Kevin Lynn, Proceedings of the SPIE, Vol. 7773, 2010.
8. Tom Stoffel, D. Renné, Daryl Myers, Steve Wilcox, Manajit Sengupta, Ray George, and Craig Turchi, *Best Practices Handbook for the Collection and Use of Solar Resource Data*, NREL Technical Report NREL/TP-550-47465, National Renewable Energy Laboratory, Golden, Co, September 2010.
9. Clifford Hansen, Joshua Stein, Steven Miller, William Boyson, Jay Kratochvil, and David L. King, *Parameer Uncertainty in the Sandia Array Performance Model for Flat-Plate Cyrstalline Silicon Modules*, Proceedings of the 37th IEEE Photovoltaic Specialists Conference (PVSC), to appear.
10. Larry Pratt and David L. King, *The Effect of Uncertainty in Modeling Coefficients Used to Predict Energy Production Using the Sandia Array Performance Model*, Proceedings of the 35th IEEE Photovoltaic Specialists Conference (PVSC), November 2010.
11. Viorel Badescu (ed.), *Modeling Solar Radiation at the Earth's Surface*, Springer, 2008.
12. D. M. Riley, C. P. Cameron, J. A. Jacob, J. E. Granata, and G. M. Galbraith, *Quantifying the effects of averaging and sampling rate son PV system and weather data*, Proceedings of the 34th IEEE Photovoltaic Specialists Conference (PVSC), February 2010.
13. http://www.nrel.gov/midc/la_ola_lanai/; data downloaded November 21, 2011.
14. Steve Ransome and Peter Funtan, *Why Hourly Averaged Measurement Data is Insufficient to Model PV System Performance Accurately*, Proceedings of the Twentieth European PVSEC, Barcelona, Spain, June 2005.
15. Nils H. Schade, Andreas Macke, H. Sandmann, and C. Stick, *Enhanced solar global irradiance during cloudy sky conditions*, Meteorologishe Zietschrift, Vol. 16, pp. 295-303, June 2007.
16. Jennifer Luoma, Jan Kleissl, and Kennan Murray, *Optimal inverter sizing considering cloud enhancement*, to appear in Solar Energy, 2012.
17. Joakim Widén, Ewa Wäckelgård, Jukka Paatero, and Peter Lund, *Impacts of different data averaging times on statistical analysis of distributed domestic photovoltaic systems*, Solar Energy, Vol. 84, pp. 492-500, 2010.

DISTRIBUTION

1   MS0899   RIM Reports Management   9532 (electronic copy)

Sandia National Laboratories